AECU-3917

WASHINGTON UNIVERSITY
Department of Chemistry

Dissertation Committee:

Joseph W. Kennedy, Chairman
Arthur C. Wahl
Samuel I. Weissman

ELECTRIC CONDUCTION IN AN OIL-PUMPED VACUUM SYSTEM

by

Ernest A. Bryant

A dissertation presented to the
Graduate Board of Washington
University in partial fulfilment
of the requirements for the
degree of Doctor of Philosophy

May, 1956

Saint Louis, Missouri

DISCLAIMER

TABLE OF CONTENTS

APPENDICES

LIST OF ILLUSTRATIONS

ELECTRIC CONDUCTION IN AN OIL-PUMPED VACUUM SYSTEM[1]

I. Introduction

Insulation has been a source of considerable difficulty for those who work with high voltages. This problem has been especially serious in electrostatic generators, and electrical leakage has limited their usefulness as particle accelerators. Workers with such instruments have always been troubled by the failure of the vacuum space as an insulator at high voltages. The cause and true nature of this leakage current is not known, and there is no successful method for its elimination.

We have investigated the leakage of electricity across a vacuum space in an electrostatic generator which employs a mixture of Sr^{90} and Y^{90} as the source of charging current. In the past, electrostatic generators employing beta-emitting isotopes have produced voltages of several hundred kilovolts.[2,3,4,5,6] If a vacuum space could be made a

---

[1]This dissertation was prepared under the direction of Dr. Joseph W. Kennedy.

[2]H. G. J. Moseley, Proc. Roy. Soc. A88, 471 (1913).

[3]U. Merten, Ph.D. Thesis, Washington University, St. Louis, (1955).

[4]P. H. Miller, Jr., Phys. Rev. 69, 666 (1946).

[5]P. V. Murphy, A.M. Thesis, Washington University, St. Louis, (1954).

[6]E. G. Linder and S. M. Christian, J. Appl. Phys. 23, 1213 (1952).

perfect insulator the voltage which could be obtained with such a current source would be limited only by the maximum energy of the beta particles. Actually the voltages have always been limited at considerably lower values apparently by leakage through the vacuum space.

We have encountered two types of voltage limitation in our system. In one case, the voltage builds up to the limiting value and then remains steady; the continuous leakage of electricity causing this limitation we call the dark current. The other type of leakage occurs as large bursts of current which reduce the voltage immediately by a number of kilovolts. This we call vacuum spark. Most of our investigation has been of the dark current.

Leakage of electricity through a vacuum space must involve the passage of at least one species of charged particle from electrode to electrode. In a discussion of vacuum conduction the mechanism for the production of the charged particles is of prime importance. There are two ways in which a charged particle can be formed in a high-voltage device such as ours. An electric field or a high temperature at one or the other of the electrodes may induce "spontaneous" emission of charged particles. Typical phenomena of this type are field emission of electrons[7,8], the "Malter" effect[9],

---

[7]W. P. Dyke and J. K. Trolan, Phys. Rev. 89, 799 (1953).

[8]R. H. Fowler and L. Nordheim, Proc. Roy. Soc. A119, 173 (1928).

[9]L. Malter, Phys. Rev. 50, 48 (1936).

field emission of positive ions[10], and thermionic emission of electrons. Charged particles can also be formed by the impact of energetic particles on an electrode surface. A typical phenomenon of this type is the production of secondary electrons at a metal surface bombarded by positive ions.[11,12,13]

It seems unlikely that field or thermionic emission of electrons or positive ions contributes to the leakage of electricity in our system. Field emission of electrons becomes important for cathode fields of about 10^7 volts cm^{-1}, and field emission of positive ions is not appreciable below about 10^8 volts cm^{-1} at the anode surface. These are a thousand times larger than the gross anode and cathode fields present in our system. Thermionic electron emission at room temperature is very much smaller than our charging currents.

The "Malter" effect[9] and related effects[5,14] can be important sources of current at gross cathode fields of about 10^5 volts cm^{-1}. The largest cathode field obtained in our system was 5×10^4 volts cm^{-1}, so it is possible that we have encountered some leakage from this type of phenomenon.

---

[10] E. W. Müller, Zeitschrift fur Physik, Bd.131, S136 (1951).

[11] A. G. Hill, W. W. Buechner, J. S. Clark, and J. B. Fisk, Phys. Rev. 55, 463 (1939).

[12] L. H. Linford, Phys. Rev. 47, 279 (1935).

[13] H. C. Bourne, R. W. Cloud, and J. G. Trump, J. Appl. Phys. 26, 596 (1955).

[14] T. J. Lewis, Proc. Phys. Soc. 68B, 504 (1955).

If the production of particles at an electrode by the impact of particles from the other electrode is to produce a leakage current there must be a continuing supply of incident particles. Spontaneous emission could provide such a continuous supply. On the other hand the production of secondary particles at both electrodes might provide a self-sustaining chain. Such a chain mechanism was proposed by Van Atta, Van de Graaff, and Barton[15]. They proposed that an exchange of particles takes place between electrodes, electrons from the cathode striking the anode to produce positive ions and photons which in turn strike the cathode to produce electrons. U. Merten[3] proposed a chain or exchange mechanism in which secondary positive ions escape from the anode surface by evaporation.

In general a self-sustaining exchange can exist only if the coefficient product, c_1c_2, is unity. Here c_1 is the average number of secondary particles produced at electrode 1 by each particle from electrode 2, and c_2 is the average number of particles produced at electrode 2 by each particle from electrode 1. Unless one of these coefficients depends upon the potential difference between the electrodes, the voltage would be limited at zero kilovolts or not limited at all by exchange. Thus it must be assumed that as the voltage increases the coefficient product increases, finally reaching unity. At this voltage a leakage current would then increase shapply and achieve whatever proportions are necessary to

---

[15]Van Atta, Van de Graaff, and Barton, Phys. Rev. 43, 158 (1933)

balance the charging current. If one or both of the coefficients are sensitive to current, the limiting voltage will depend on the amount of charging current, and the leakage current may be appreciable well below the limiting voltage.

In leakage of this type it is possible that a large fraction of the current can be carried by particles which do not contribute significantly to the maintenance of the chain. For example, two possible secondary cathodic particles are electrons and negative ions; the negative ions may be the principal producers of the anodic particles, but the electrons may be much more numerous. Thus in an investigation of an exchange mechanism the discovery of a current carrier does not mean that a member of the exchange-chain has been found. In a study of current loading in ion accelerating tubes McKibben and Boyer[16] found that although electrons carried 98 per cent of the leakage current, the threshold voltage for exchange was not affected by a magnetic field which prevented the electrons from reaching the anode.

Little is known about the actual values of coefficients which might be of interest in a study of exchange leakage. Some investigations have been made of the number of electrons produced by positive ions such as H^+, He^+, Ne^+, N_2^+, A^+, and Hg^+. These experiments have been made mostly with thoroughly cleaned and outgassed metal targets.[10,11,12] It has generally been found that between 2 and 20 electrons are

---

[16] J. L. McKibben and K. Boyer, Phys. Rev. 82, 315A (1951)

produced by a 100-kev positive ion. In most cases the coefficient has been found to increase only slowly with anode voltage from one hundred to several hundred kilovolts. A recent paper[13] reports a linear increase in coefficient for helium ions on a copper target from 20 to 140 kilovolts accelerating voltage.

Nothing is known of the coefficients for production of negative ions by anodic positive ions in the energy region of interest. McKibben and Boyer[16] propose a negative ion-positive ion exchange but make no estimates of the coefficients. The work of Sloan[17] and Arnot[18] indicates that there is a finite probability for such a reaction. They found that a spectrum of negative ions was formed by the impact of a single species of positive ion, and that the coefficient might be very roughly 10^{-4} negative ion per positive ion, this at accelerating voltages of only a few kilovolts. The ratio of negative ions to positive ions produced by electron bombardment of organic vapors in mass spectrometers[19,20] is usually less than 10^{-2} ; in such cases the most abundant of the negative ions is hydride ion.

Coefficients for the production of positive ions by electrons have been found to be very sensitive to surface contamination.[21]

---

[17] R. H. Sloan and R. Press, Proc. Roy. Soc. A168, 284 (1938).

[18] F. L. Arnot and C. Beckett, Nature 141, 1011 (1938).

[19] L. G. Smith, Phys. Rev. 51, 263 (1937).

[20] H. O. Pritchard, Chem.Rev. 52, 529 (1953).

[21] I. Filosofo and A. Rostagni, Phys. Rev. 75, 1269 (1949).

Experimental values from 10^{-6} to 10^{-3} have been obtained for the yield of positive ions per incident electron.[16,21] There are no experiments on the production of positive ions by incident negative ions.

The leakage current in our system, as we shall see later, is carried largely by electrons and positive ions. However no definite conclusions can be drawn from the data available in the literature as to whether or not an exchange is possible involving electrons, negative ions, or both as the cathodic particles. We believe that such a mechanism, involving both electrons and negative ions, is responsible for the leakage in our system.

II. Experimental

Vacuum system

All experimental work was done in a cylindrical metal vacuum chamber, figure 1. An anode, a, containing the beta-emitter, is supported on a quartz rod, q, which is mounted on a grounded metal plate in the lower part of the vacuum chamber. The vacuum chamber is constructed of brass, except for the aluminum top. The inner surface of the cylindrical section is tinned with solder. Joints are sealed with neoprene O-rings greased with either Apiezon-N or Airco Hy-Vac stopcock grease. A 0.01-inch aluminum foil, i, permits measurement of the beta-ray intensity at the cathode. A glass port, p, on one side is used for visual observations. With the glass removed, positive ion counting apparatus may be attached at this point. On the opposite side a projection contains an alpha-particle counter, f, and an air absorption tube, t. Distributed around the bottom are a number of electrical lead-throughs, e, an ionization gauge tube for pressure measurements, and a stopcock.

A Duo-Seal Vacuum Pump (No. 1402B) , with a free air capacity of 140 liters per minute, is used as a fore-pump. A D.P.I type MCF-60 oil diffusion pump is used between the fore-pump and the vacuum system. Both Octoil-S and DC-703 silicone oil have been employed as the pump oil in the diffusion pump. A water cooled baffle plate, b, provides trapping between the diffusion pump and the vacuum line. During

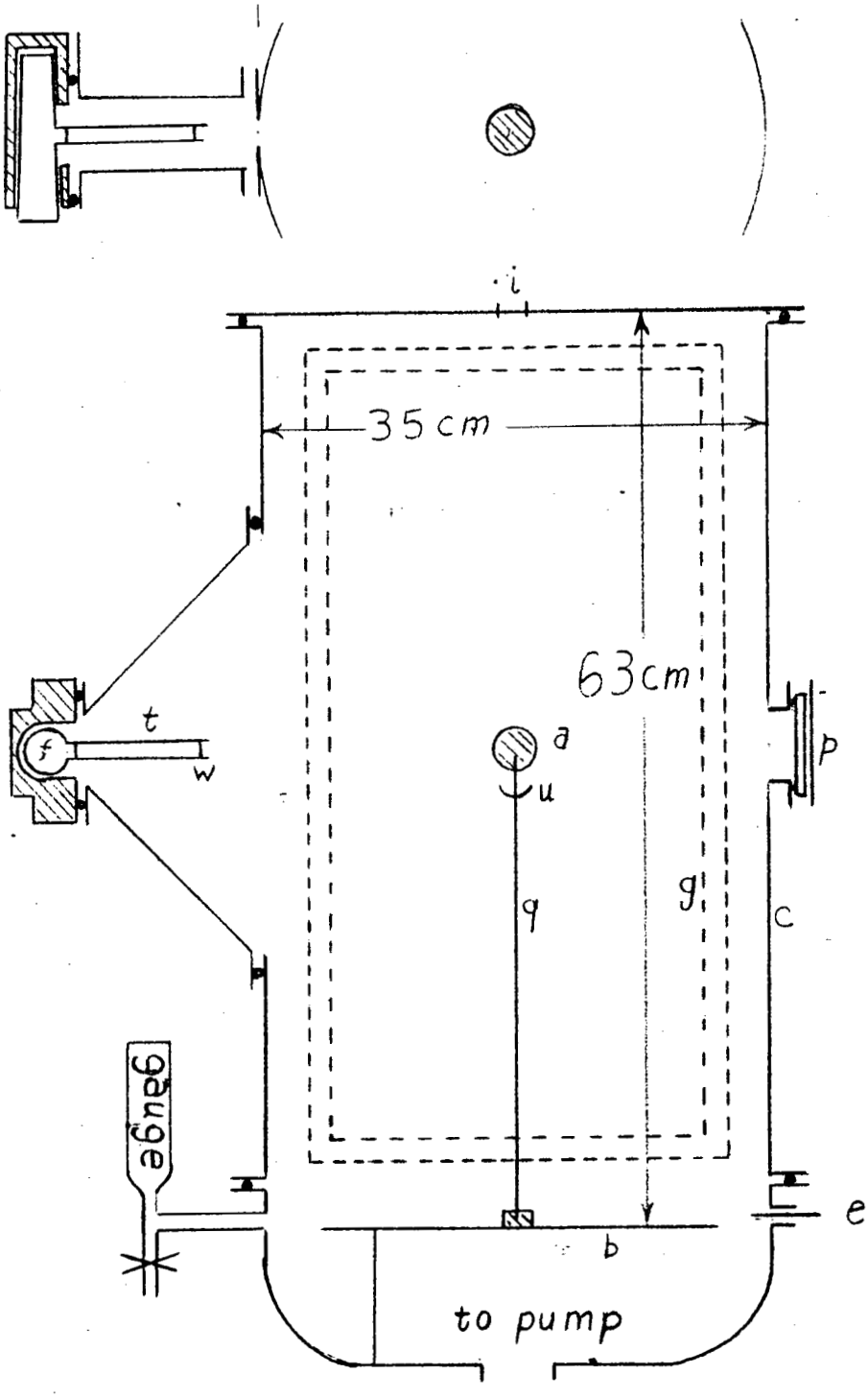

FIGURE 1

Vacuum Chamber

experiments the pressure was ordinarily maintained at 5×10^{-6} mm Hg.

Three anodes were employed (figure 2), 1, 2.5, and 4 centimeters in diameter. These were machined from stock aluminum metal. The anodes are so constructed that a beta source, S, will fit inside. The beta particles shine out through a 0.002-inch window, W. Each of the two smaller anodes has a recess in one side in which an alpha source is placed.

The supporting rod, q (figure 1), was made from either 3 or 5-millimeter quartz rod. In some cases an inverted umbrella-like quartz projection, u, was provided close to the anode end of the rod. A grid structure, g, will be described later.

The aluminum anodes were cleaned with detergent, distilled water, and reagent grade acetone before assembly of the system. The rods were cleaned with chromic acid, distilled water, and reagent grade acetone.

The beta sources contain a mixture of strontium-90 and yttrium-90 in secular equilibrium. Sources of three different strengths were employed. The strengths, in terms of effective micromicroamperes of changing current at zero voltage, are 15 ($\mu\mu$a), 50 ($\mu\mu$a), and 180 ($\mu\mu$a). These beta sources were prepared as follows. A 0.005-inch stainless steel sheet was soldered to a 0.025-inch soft iron sheet. Disks, 3/8 inch in diameter, were stamped from the resulting sheet. A solution containing the mixture of strontium and yttrium was obtained from the Isotopes Division, U.S.A.E.C., Oak Ridge, Tennessee. The strontium was purified, when necessary, by

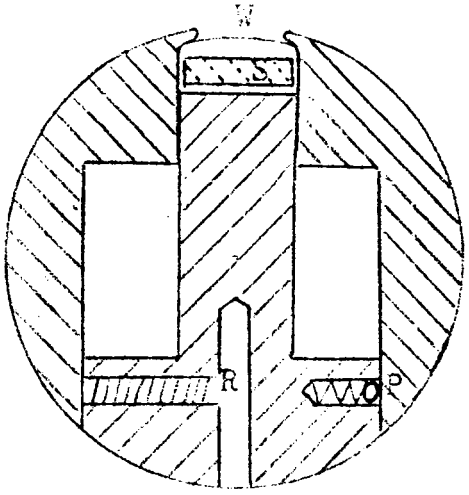

4-cm Anode

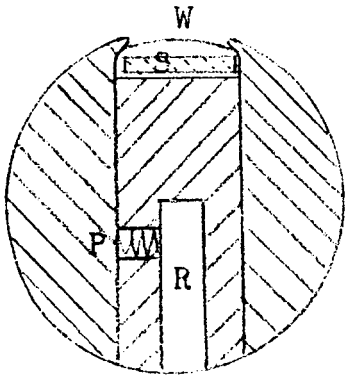

2.5-cm Anode

W- Thin window

S- Beta source

R- Hole for supporting rod

P- Spring

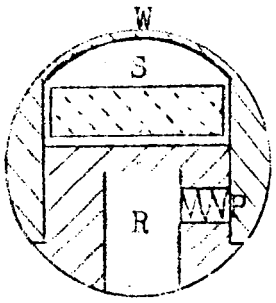

1-cm Anode

FIGURE 2

ANODES

precipitation as the carbonate followed by re-solution in nitric acid. The solution was placed, a drop at a time, on one of the disks and evaporated to dryness with a heat lamp. The entire disk was then "canned" in nickel by thermal decomposition of nickel carbonyl. This gave an airtight coating, approximately 0.001 inch thick, which served to isolate the active deposit.

Alpha sources were prepared by hydrogen deposition of about 1 millicurie of polonium-210 from a slightly acid solution onto a paladium foil a few square millimeters in area.

Voltage determination

The electric potential of the anode was determined by measuring the change in the range of alpha particles emanating from a source of polonium-210 on the anode. Thus alpha particles from the anode, a (figure 1), are accelerated across the vacuum space and enter an air absorption tube, t, through a mica window, w. They then pass through a second mica window and are detected in a flow proportional counter, f. The range is determined by varying the pressure in the adsorption tube and extrapolating a graph of counting rate versus pressure to zero counting rate. The range is determined with the anode at voltage and again with the anode at ground potential. The differences in range are converted to differences in energy by use of published range-energy data.[22] Division of the energy difference, expressed in electron volts, by two gives the anode potential in volts.

A second, more rapid method for determining the anode

---

[22] H. A. Bethe, Rev. Mod. Phys. 22, 213 (1950).

voltage depends on calibration of the current output of an ionization chamber placed above the aluminum foil, i (figure 1), against voltage as determined by alpha range measurements. Figure 3 illustrates a typical calibration curve.

An independent check on voltage measurements was provided by electric field deflection of a beam of positive ions originating at the anode. All ions with the same energy-to-charge ratio are deflected a like amount by an electric field. Voltages calculated from the deflection of this beam of ions agreed with voltages determined by alpha range measurements within about 10 kilovolts.

Recording system

A grid structure (figure 4), consisting of two concentric grids, was used in most experiments. The inner grid (called grid 2) is made of 0.005-inch nichrome wires spaced about $\frac{1}{4}$ inch apart. Grid 2 is composed of five sections; the top, the bottom, and three equal cylindrical sections, each of which occupies 120° of the circumference. The outer grid (grid 1) is made of hardware cloth which has approximately three wires per inch in both directions. This grid is composed of three sections; the top, the bottom, and the cylindrical section. The two grids are separated by 5/8 inch, and grid 1 is about 1-3/8 inch from the wall of the vacuum chamber. The screening fraction of grid 1 is approximately 0.25. The wires of grid 2 cover 0.02 of the area of the grid, and the supporting structure covers about 0.02, making a total screening fraction of about 0.04.

Bias voltages are supplied to the grids through d.c.-

FIGURE 3

CALIBRATION OF IONIZATION CHAMBER

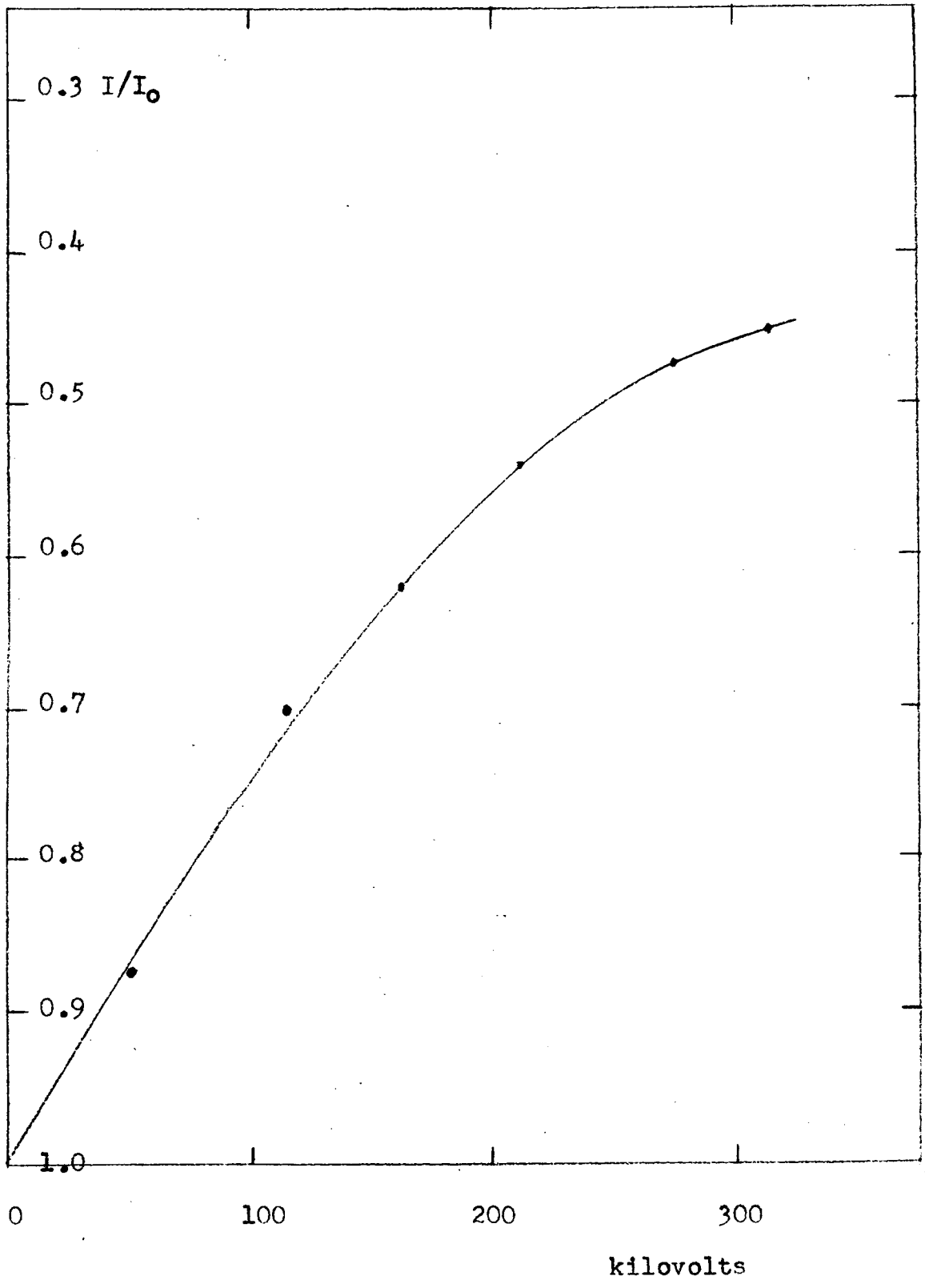

GRID SYSTEM

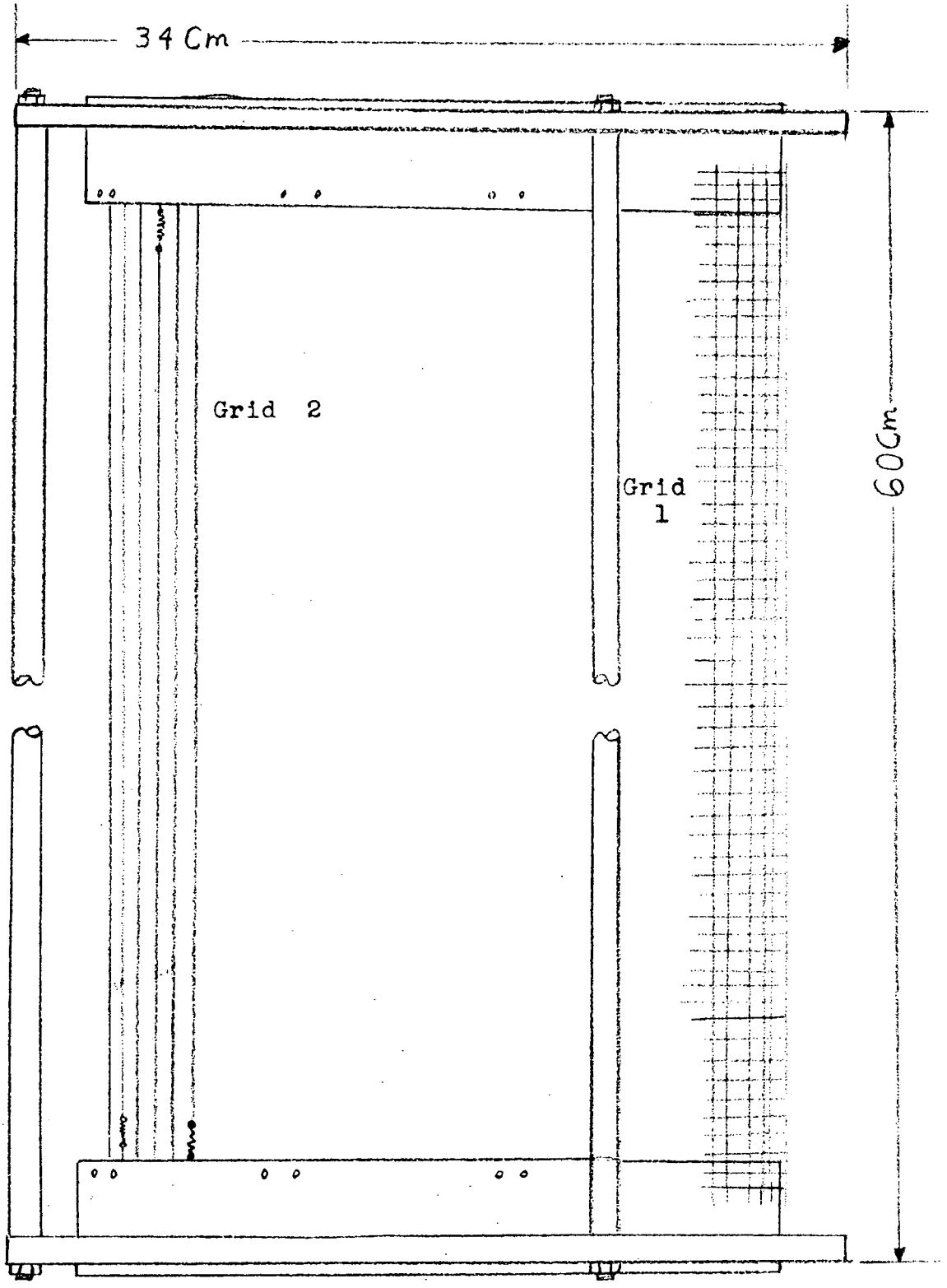

FIGURE 4

shielded lead-throughs. The bias voltages are obtained by connecting the desired number of 300-volt batteries in series. Figure 5 is a schematic diagram of the electrical system.

An automatic device records currents passing to the grids, as well as the current in the ionization chamber. (Figures 5, 6, 7, 8, and 9). A switch box contains relays to select the channel, resistors to convert currents to voltages, and capacitors to store sudden bursts of current. The voltage from this box is fed to the input terminal of a Cenco "Electronic Electrometer".[23] This electrometer has an input resistance of about 10^{15} ohms and is capable of measuring voltages from 0 to 5 volts or from (-)2.5 to (+)2.5 volts. The voltage appearing across the terminals of the meter in the electrometer is amplified and converted to a current. This current is then used to drive an Esterline-Angus recorder.[24] The relays which select the proper channel are controlled by a stepping switch which in turn is activated by a micro switch on the chart drive mechanism of the recorder. Each channel is recorded for a period which is some multiple of 30 seconds. The most common practice was to record grid currents for thirty seconds each and ionization chamber current for 60 seconds.

A difference amplifier (figure 7) is used to control a relay which connects a 4-micromicrofarad capacitor across the input of the electrometer when positive or negative pulses larger than 2.5 volts in magnitude appear at this terminal.

---

[23]Catalog No. 71010, Cenco Scientific Co. 1700 Irving Park Road, Chicago.

[24]0-1 ma recorder, Model No. AW., Esterline-Angus Co., Indianapolis.

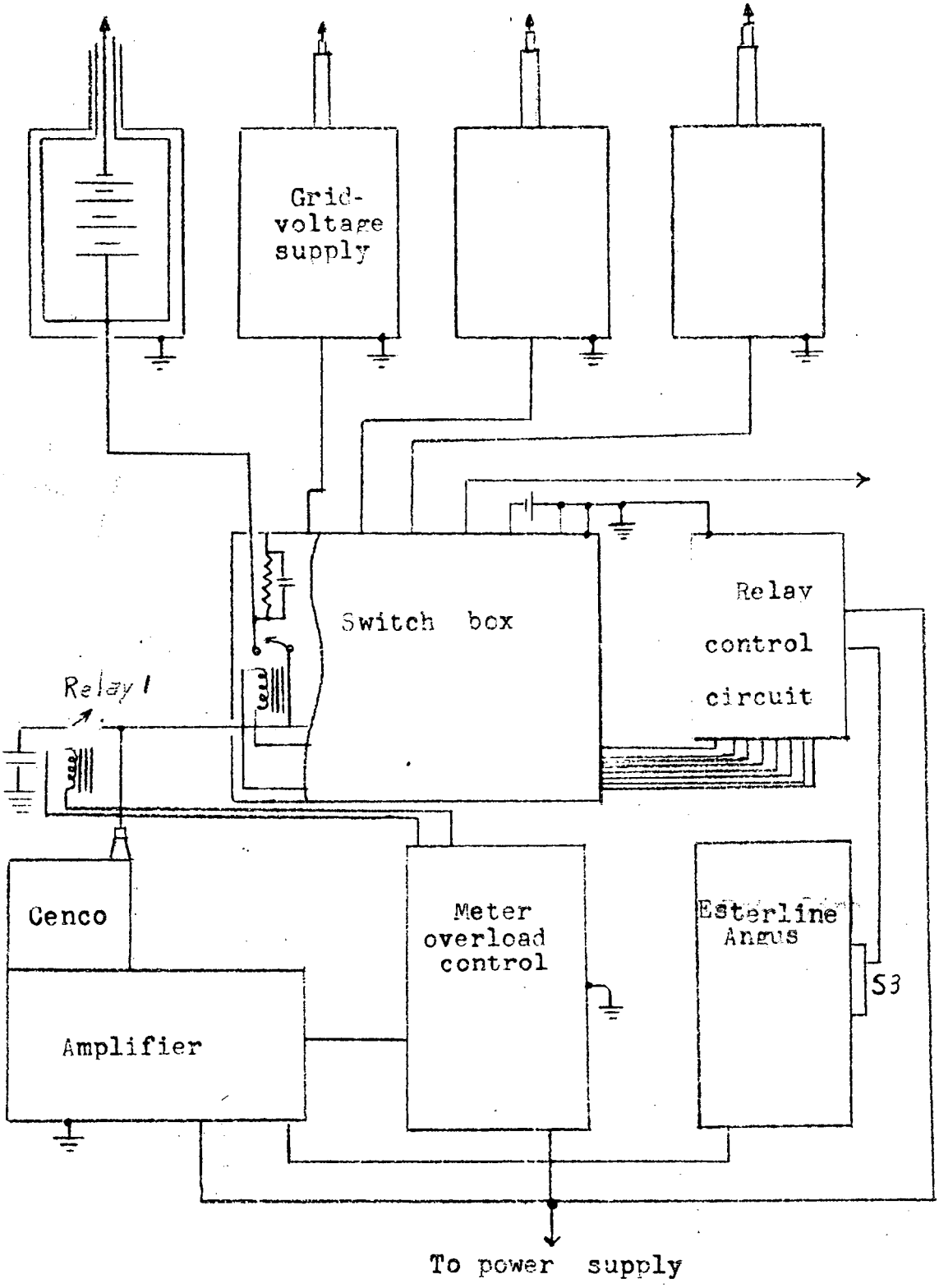

FIGURE 5

Recording System

FIGURE 6

Amplifier

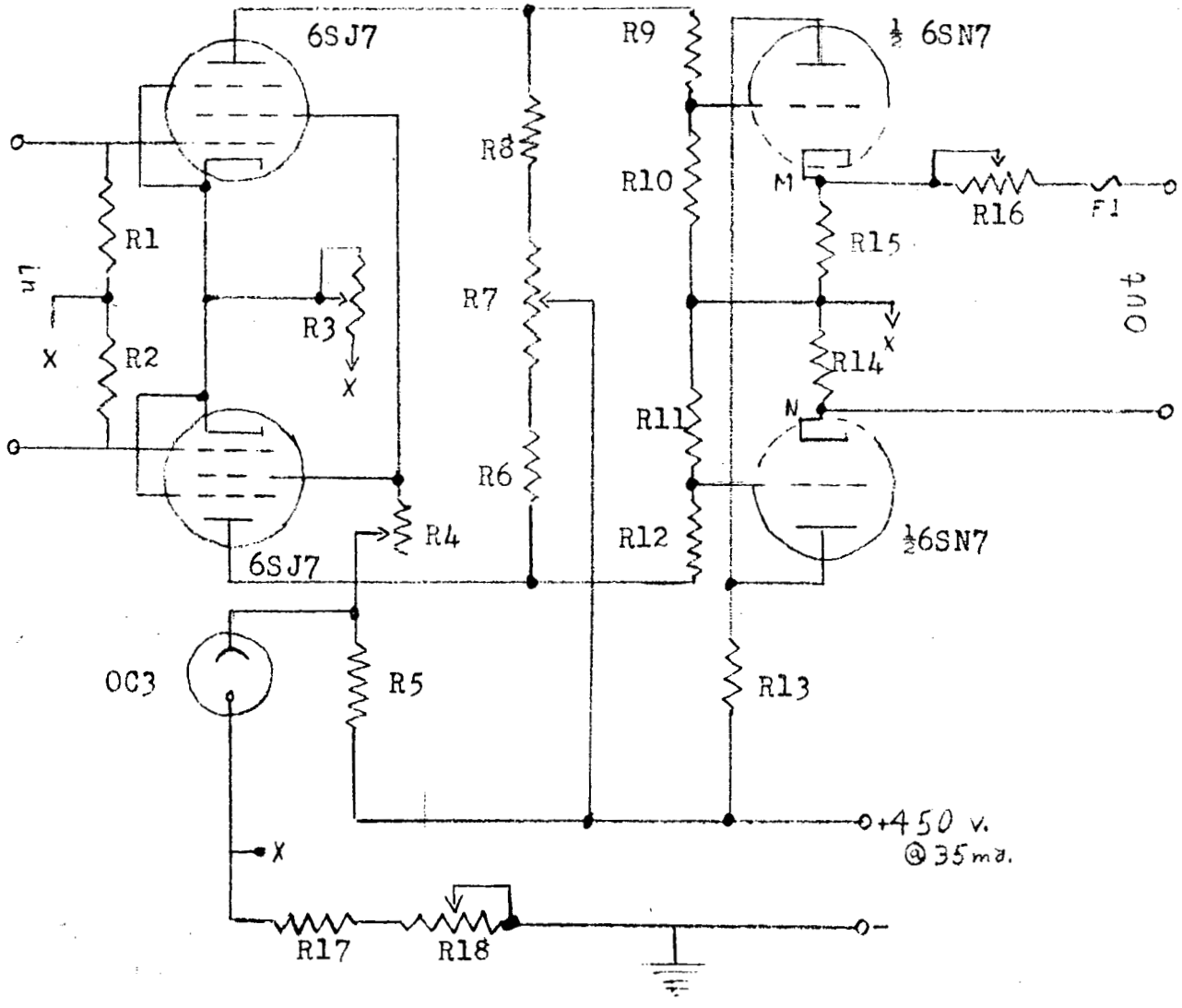

Figure 7

Difference Amplifier

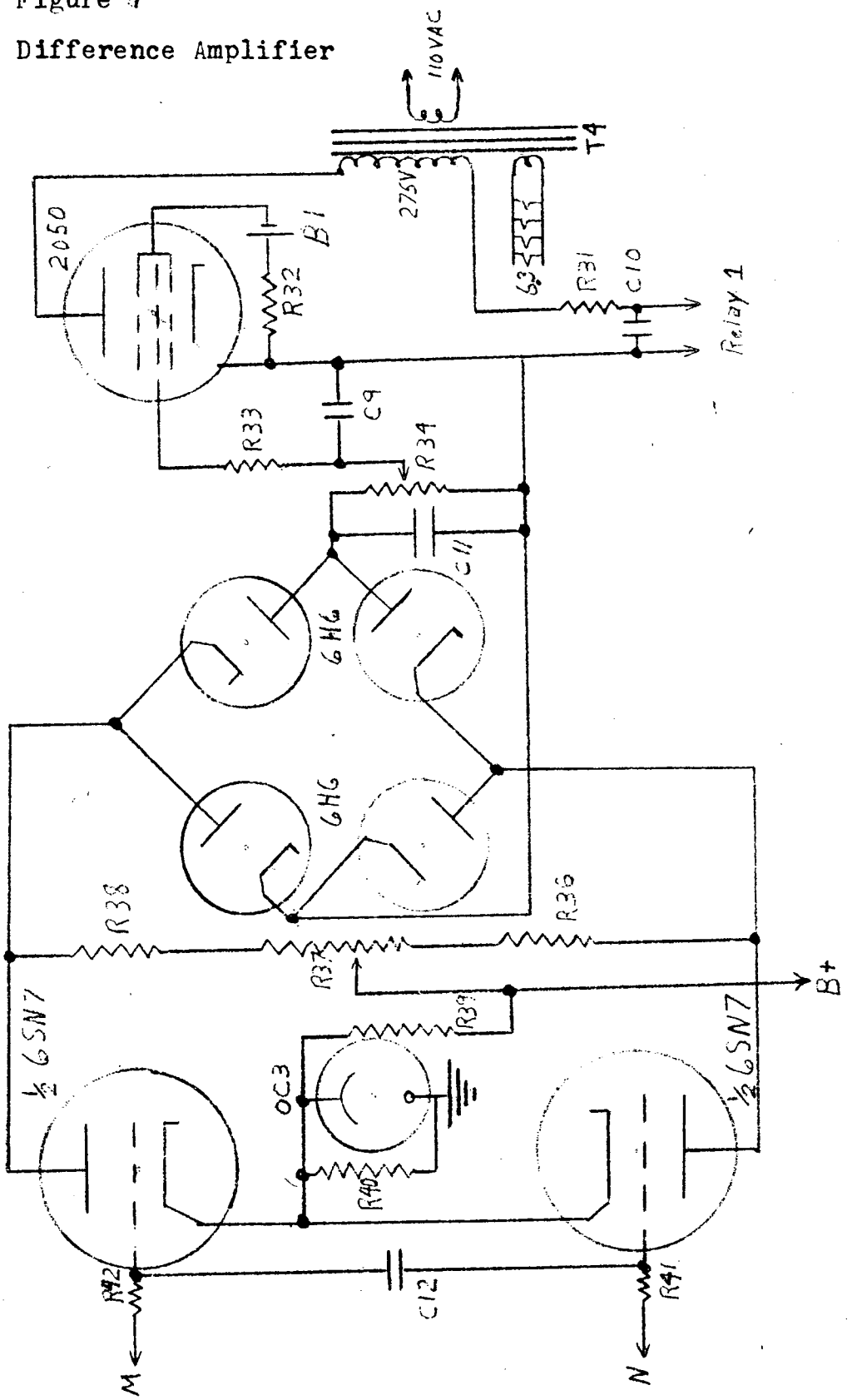

FIGURE 8

Channel Selector

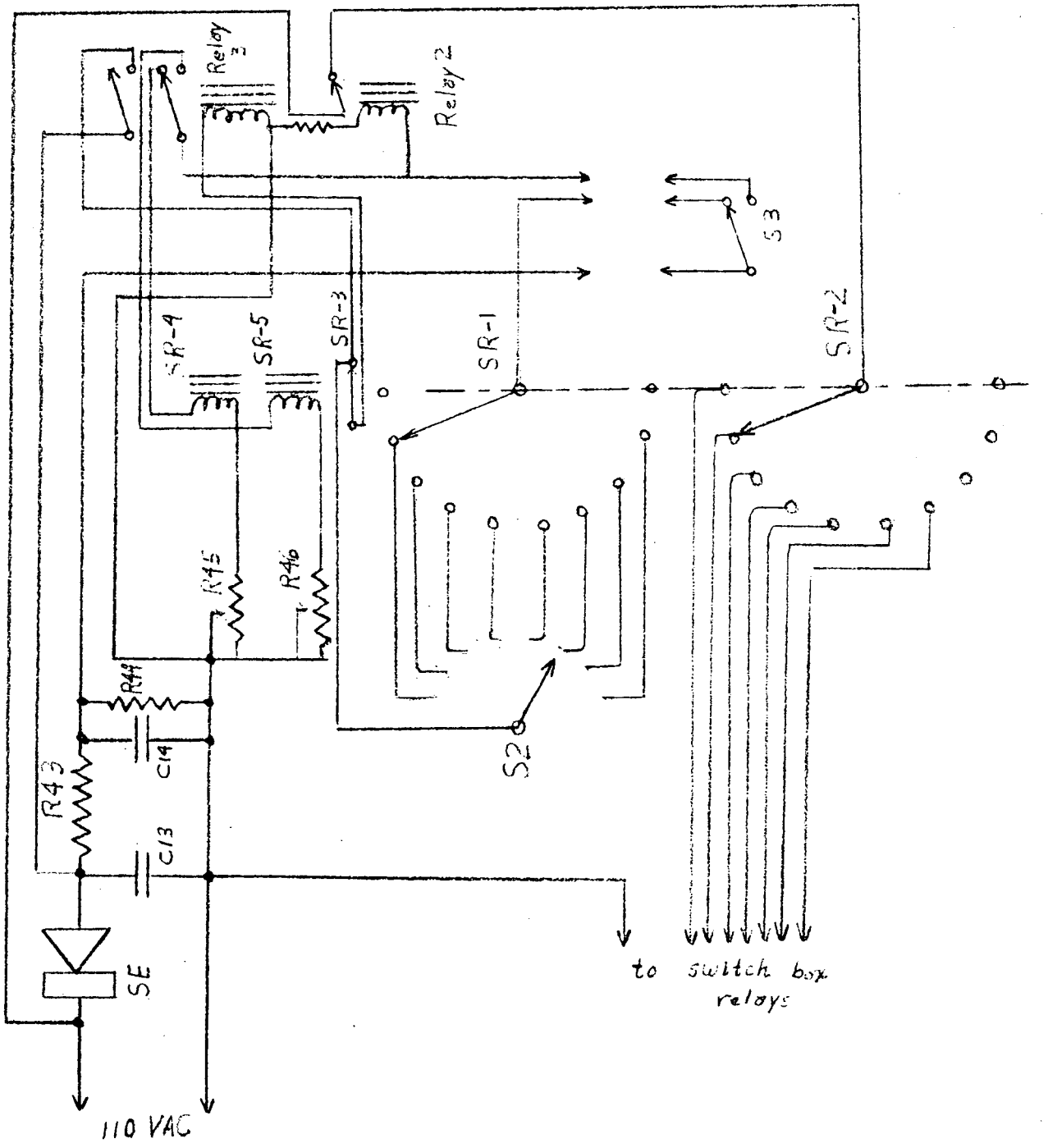

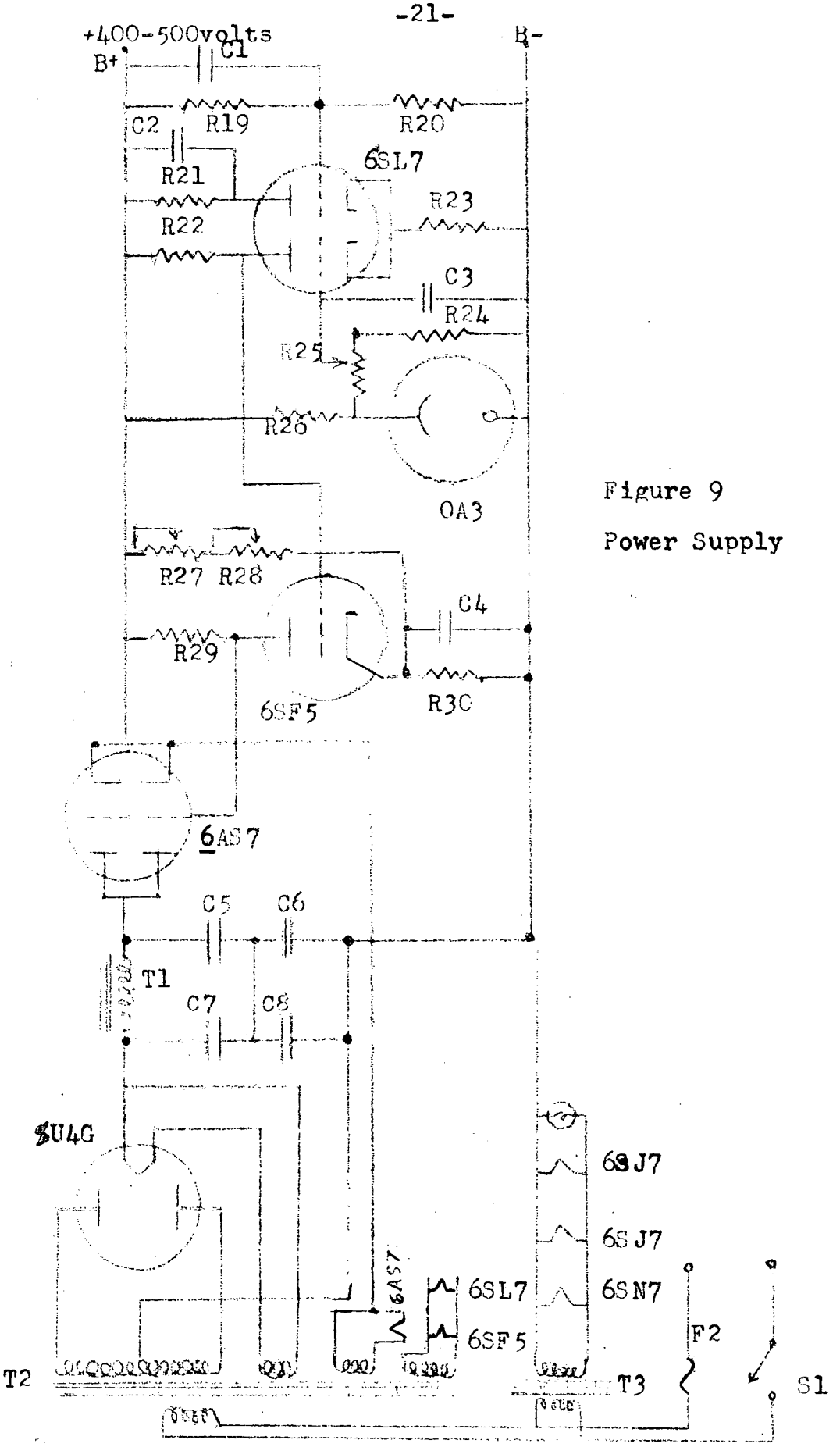

Figure 9

Power Supply

Components of the Electrical System

R1,2	0.15 meg, 1%	R32	100 k
R3	100 ohm, 10 watt	R33	1 meg
R4	10 k pot.	R34	1 meg pot.
R5	33 k , 2 watt	R35	(deleted)
R6,8	40 k, 5 watt, 5%	R37	20 k pot.
R7	3 k pot.	R36,38	47 k, 2 watt
R9,12	160 k, 1%	R39	40 k, 2 watt
R10,11	120 k, 1%	R40	4 k, 5 watt
R13	8.5 k, 1 watt, 1%	R41,42	470 k
R14,15	15 k, 1 watt, 1%	R43	2.5 k, 5 watt
R16	2 k pot.	R44	4 k, 5 watt
R17	150 ohm, 1 watt	R45,46	125 ohm, 25 watt, adjustable
R18	200 ohm pot.	C1	30 mfd, 300 v
R19	390 k, 1%	C2	40 mfd, 300 v
R20	47 k, 1%	C3	15 mfd, 300 v
R21	65 k	C4	60 mfd, 300 v
R22	600 k, 1%	C5,7	30 mfd, 450 v
R23	18 k, 1 watt, 1%	C6,8	30 mfd, 450 v
R24	25 k	C9	0,1 mfd
R25	50 k pot.	C10	100 mfd, 300 v
R26	25 k	C11	10 mfd, 50 v
R27	250 ohm,adjustable	C12	0.001 mfd
R28	15 k adjustable, 10 watt		
R29	200 k, 1%	C13	50 mfd, 250 v
R30	7.5 k, 5 watt	C14	40 mfd, 250 v
R31	4 k, 5 watt		

Components of the Electrical System

F1 5 ma fuse

F2 3 ampere fuse

T1 UTC #29, 10 h, 175 ma

T2 Stancor PC-8414, 1200 v, 200 ma

T3 Sola constant voltage transformer

T4 Thordardson transformer

Relay 1 SPDT, 5 k coil

Relay 2 SPDT, 5 k coil

Relay 3 DPDT, 5 k coil

Switch box relays SPST, 110 VAC coil

SR "Minor" stepping relay

SR-1 bank 1 of stepping relay, non-shorting

SR-2 bank 2 of stepping relay, non-shorting

SR-3 (open in position 1 only)

SR-4 stepping coil

SR-5 release coil

S1 line switch, toggle

S2 Single pole 10 position rotary switch

S3 micro switch, SPDT

SE "General" selenium rectifier, 500 ma

This device, in conjunction with the capacitors in the switch box, can provide measurements of the coulomb content of bursts of current picked up by the grids.

Victoreen "Hi-Meg" resistors[25] are used in the switch box. For a particular channel a resistor was chosen so that the voltage drop across it was between 0.1 and 2.5 volts. Depending on the circumstances this was 10^9 to 10^{12} ohms. A capacitor was then chosen so that the RC time of the resistor-capacitor combination was approximately equal to the time required for the recording system to go through a complete cycle of operation.

Tests were made with high voltages on the grids to determine whether any extraneous leakage currents were being measured. Such leakage currents were always less than one micromicroampere.

Positive ion detector

An electron multiplier used for detection of positive ions is illustrated in figure 10. This device was constructed according to a design by Allen.[26] Inductive heating was employed to activate the dynode surfaces. After about two months of use the amplification factor of the multiplier had stabilized at about 10^5, and no further treatment was applied. The chamber containing the multiplier is composed of brass, and the joints are sealed with neoprene O-rings. High voltage

---

[25]The Victoreen Instrument Co., 5806 Hough Ave., Cleveland

[26]J. S. Allen, Rev. Sci. Instr. 18, 739-49 (1947).

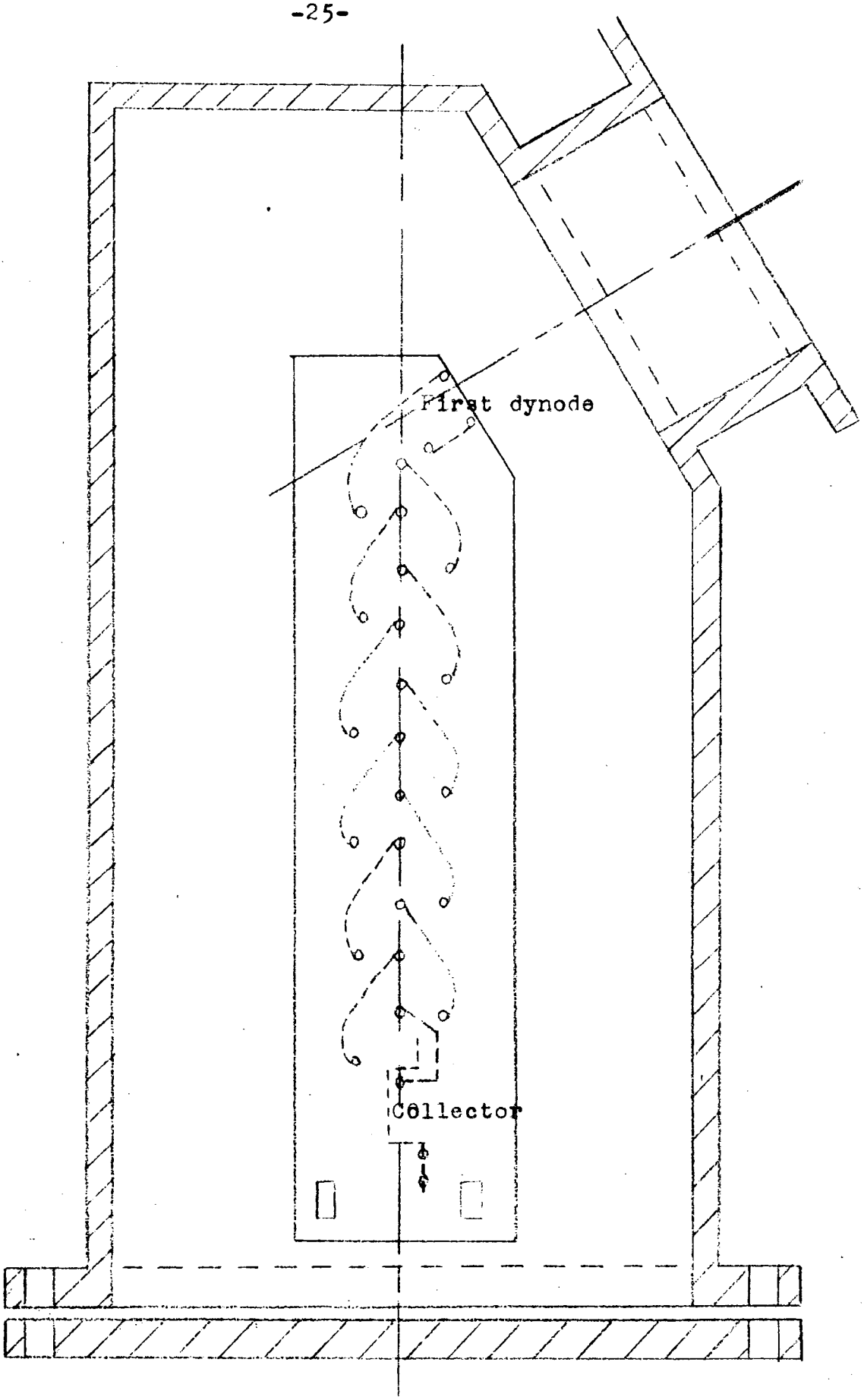

FIGURE 10 ELECTRON MULTIPLIER

for the operation of the electron multiplier is obtained from a 0-7000 volt regulated supply. The normal operating voltage was 5,200 volts.

The pulses produced by the electron multiplier were detected and counted with a conventional system employing Atomic Instrument Co.[27] preamplifier (model 219), amplifier (model 218), and scaler (model 131). A counting rate computer[28] was sometimes used to record counting rate data on the Esterline-Angus recorder.

A mass spectrometer (figures 11 and 12) was constructed using the electron multiplier as a detector, and one of three different permanent magnets for the deflecting field. The device is operated by raising or lowering the detector in small increments and plotting the counting rate of positive ions against vertical displacement. The spectrometer was calibrated by using polonium-210 as a source of particles with known energy and known mass-to-charge ratio.

Parallel metal plates, one above and one below the path of the positive ions (figure 12), serve as electric field deflectors of the positive ions. Electric deflection was used both to extend the range of the mass spectrometer and to provide a measure of the energy of the ions.

A Faraday cage, illustrated in figure 13, was used in conjunction with the electron multiplier to determine the

---

[27]Atomic Instrument Co., Cambridge, Massachusetts.

[28]Berkeley Scientific Co (model 1600), Richmond, Calif.

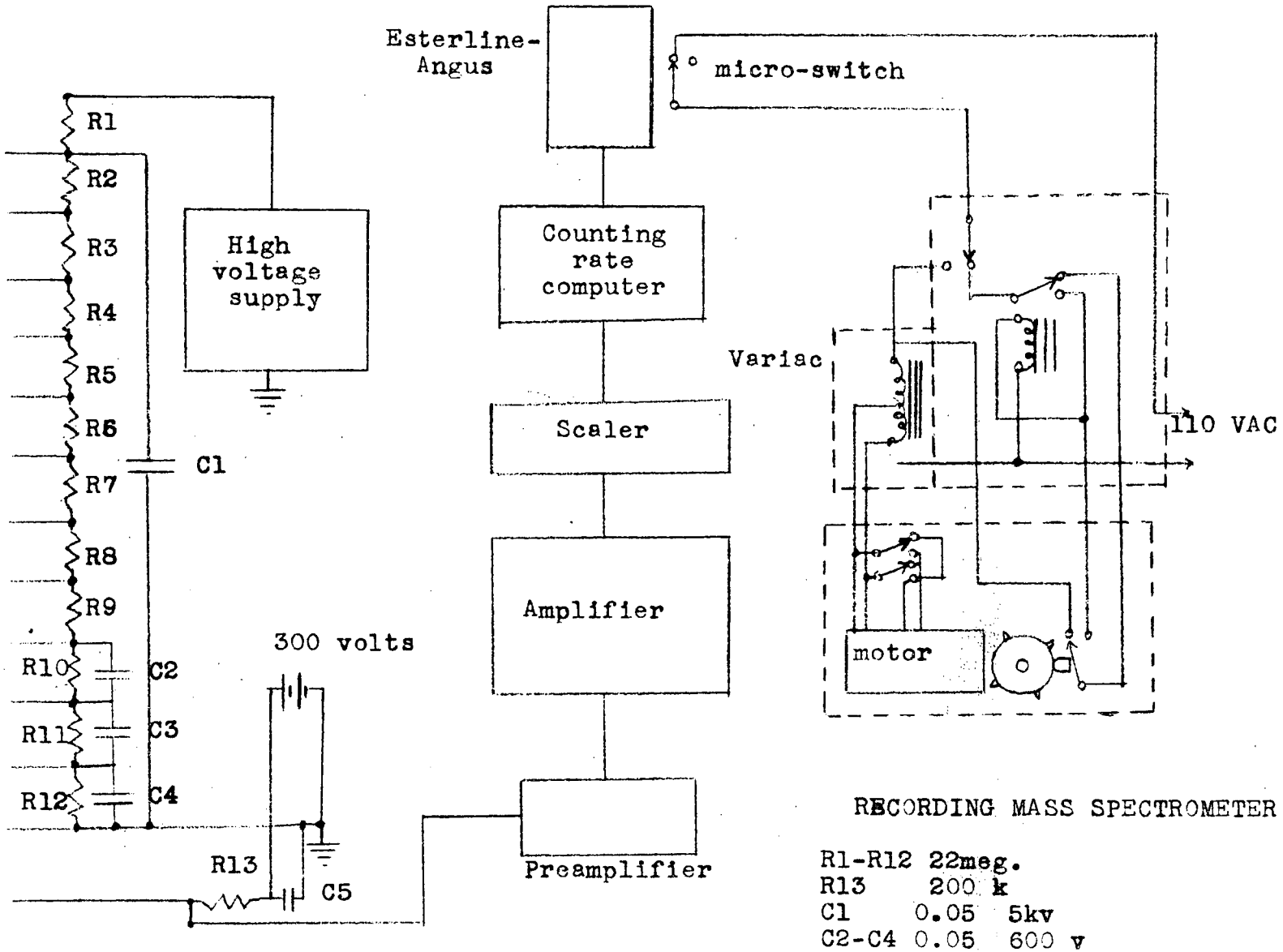

RECORDING MASS SPECTROMETER

R1-R12 22meg.
R13 200 k
C1 0.05 5kv
C2-C4 0.05 600 v
C5 0.005

FIGURE 11

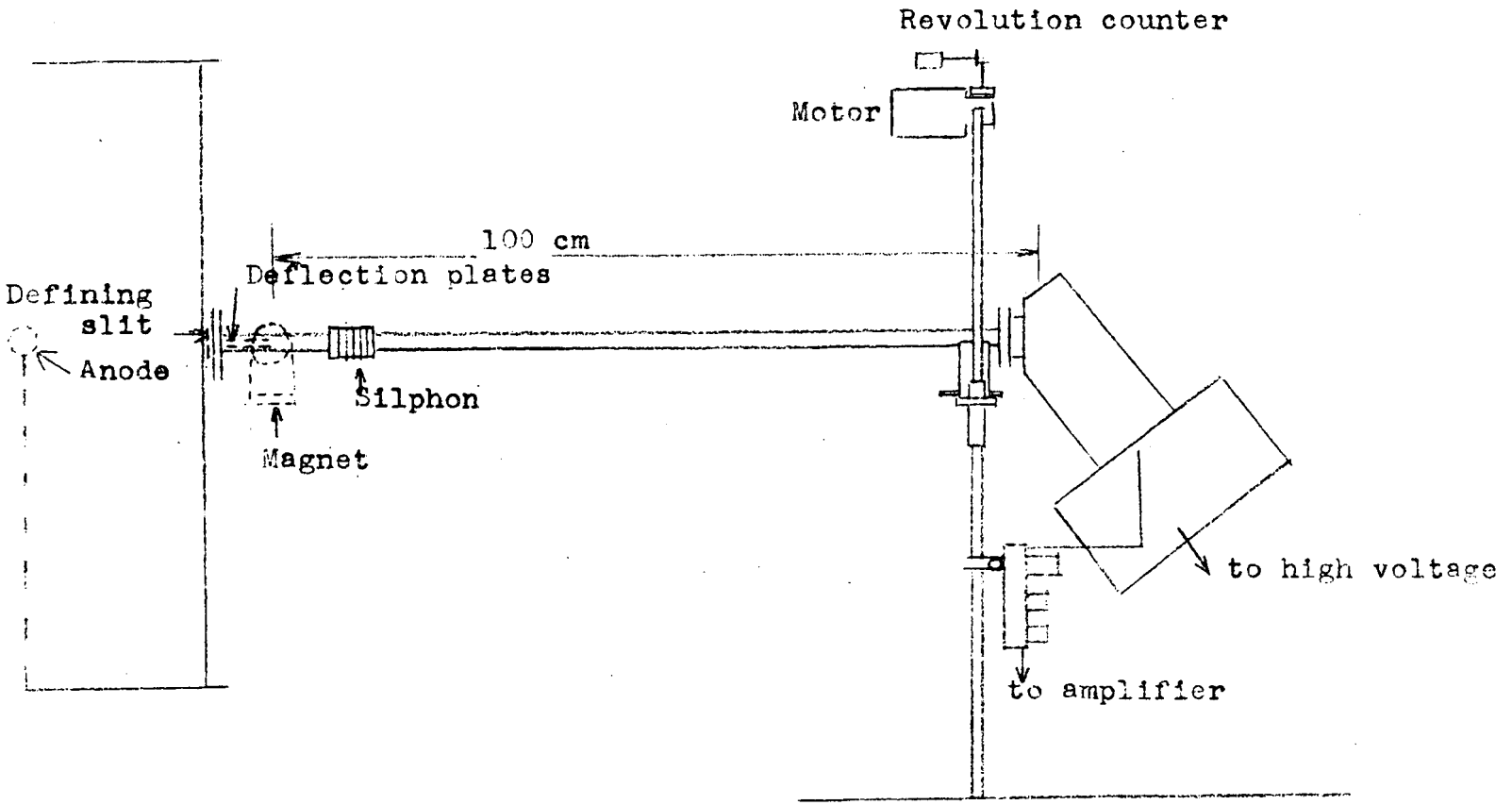

MASS SPECTROMETER

FIGURE 12

FIGURE 13

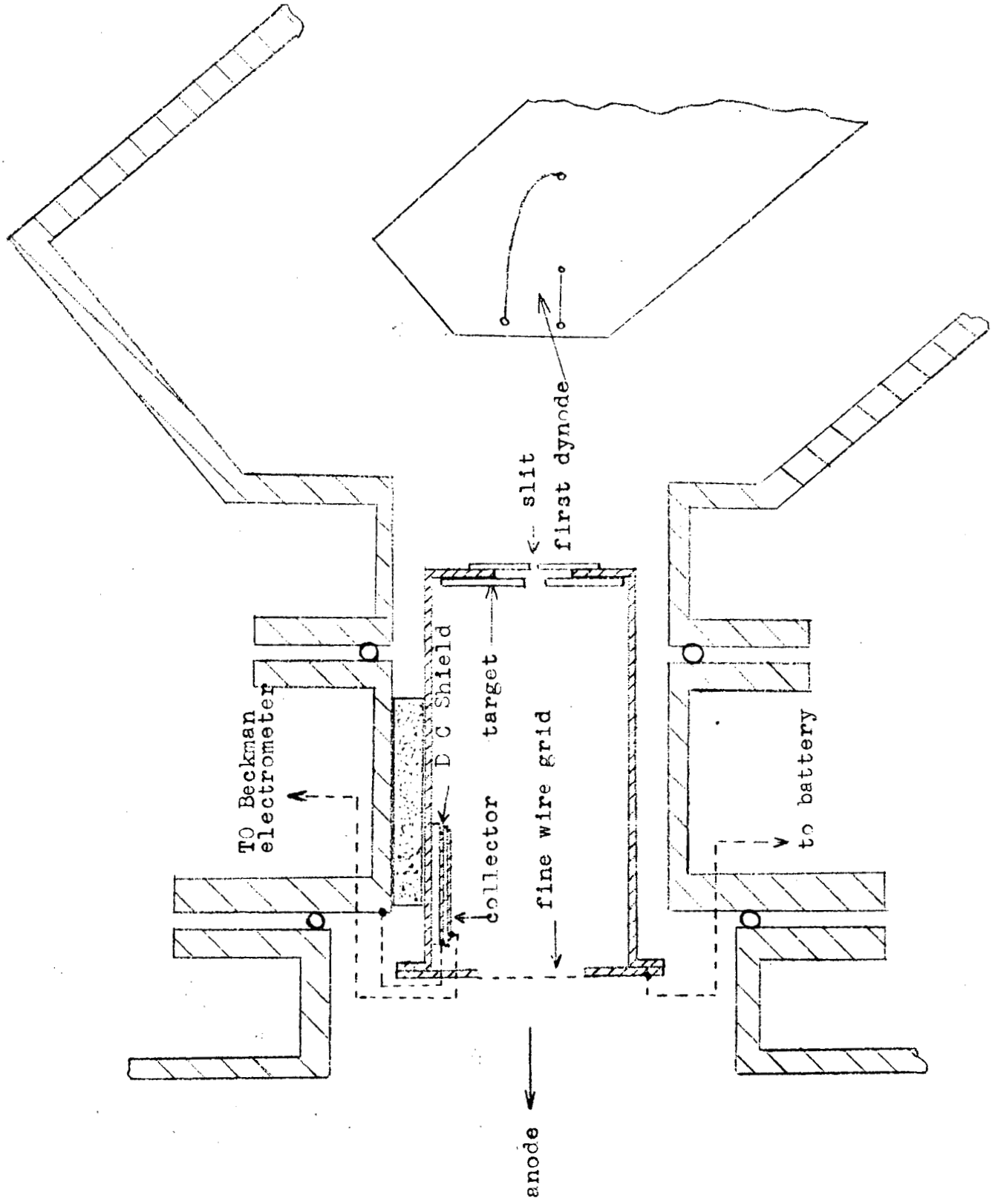

Faraday Cage for Coefficient Determinations

yields of secondary electrons and of secondary positive ions per incident high-energy positive ion. The effect of target material was determined by placing various materials in the rear of the cage. A small slit, 0.5 inch by 0.016 inch, allows one-eightieth of the positive ions which enter the cage to pass through to the electron multiplier. Charged particles produced in the cage are collected on a collector plate which is maintained at ground potential. Potential differences to facilitate the collection are provided by biasing the cage positively or negatively.

Solenoid winding

For a few experiments one hundred turns of wire were wound around the cylindrical section of the vacuum system. Ten amperes of electrical current passing through this winding produced a magnetic field of about 20 gauss parallel to the axis of the system.

III. Experimental Results

In some cases[7,8] the potential gradient at an electrode surface has been found to be an important factor in electrical leakage across a vacuum space. A summary of the potential gradients as a function of anode potential, V, at the various electrodes in our system is presented in table 1. The numbers were obtained by the assumption that the field at the cathode is the same as the field at a spherical cathode of the same diameter. A test of the validity of this approximation was conducted in an electrolytic bath with geometry similar to that of our vacuum system.[29] Table 2 presents the data from this test. The field at the grid wires was obtained by multiplying the field at a cathode of that radius by the ratio of the total cathode surface to the total surface area of the wires.

Table 1

Anode radius	Anode field	Grid 2 radius	Grid 2 field	Cathode radius	Cathode field*
0.5 cm	2.1 V cm^{-1}	13.4 cm	0.06 V cm^{-1}	17.5 cm	0.0017 V cm^{-1}
1.25	0.87	13.4	0.16	17.5	0.0044
2.0	0.59	13.4	0.27	17.5	0.0074

[29] This experiment was performed by Mrs. Joan Tuttle.

*The cathode field given in this table refers to cases in which the grid system has been removed.

Table 2

Anode radius	Cathode radius	Cathode gradient	
		measured	calculated
0.9 cm	17.4 cm	0.0034 V cm^{-1}	0.0031 V cm^{-1}
0.9	4.8	0.069	0.048

Two types of voltage limitation are encountered in our system. The first is characterized by spark discharges, the second by a steady leakage of current through the vacuum space at a limiting voltage. In the following we will describe some of the features of these voltage limitations.

Limiting voltages

For a given anode size and shape two factors which are important in determining the limiting voltage are charging current and grid bias. In figure 14 limiting voltage is plotted as a function of the voltage on grid 2. Three anodes and three charging currents are represented. In figure 15 the log of limiting voltage at high grid bias is plotted against the log of charging current. The charging current has been corrected for those beta particles which have insufficient energy to traverse the voltage gap between anode and cathode. This correction was made by the assumption that the ion chamber current is proportional to the beta flux at the cathode. The slope of the lines in figure 15 indicate an approximate relation $I=kV^{3.4}$, where V is voltage and I is leakage current.

Grid currents

The two grids, grid 1 biased positively and grid 2

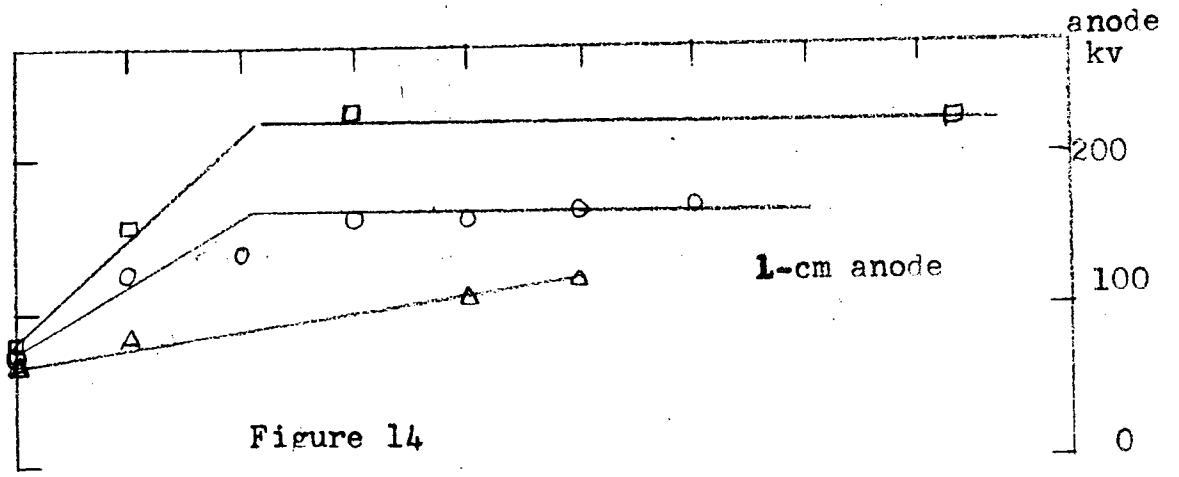

Figure 14

Voltage vs Grid-2 Bias

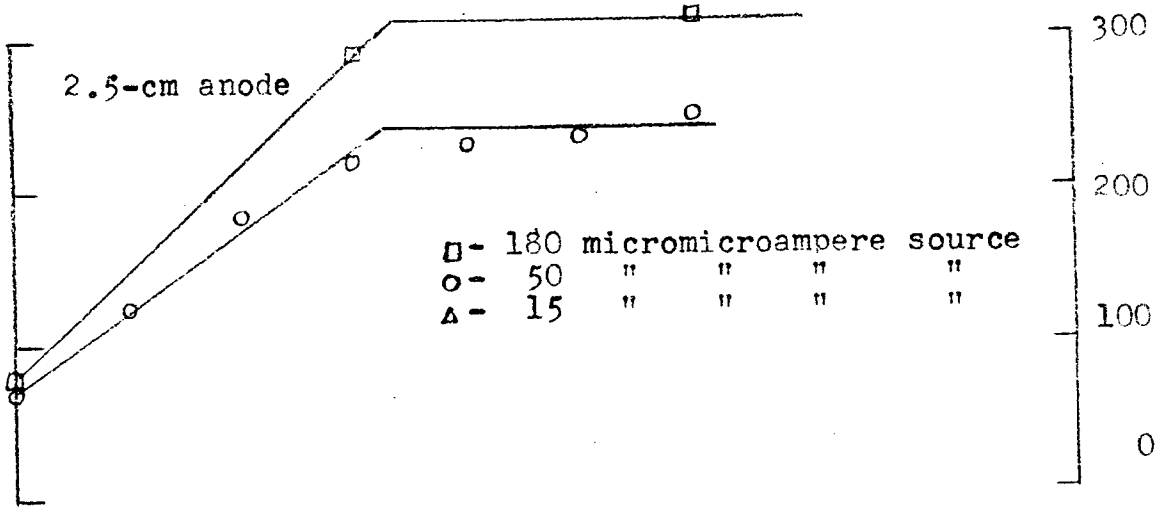

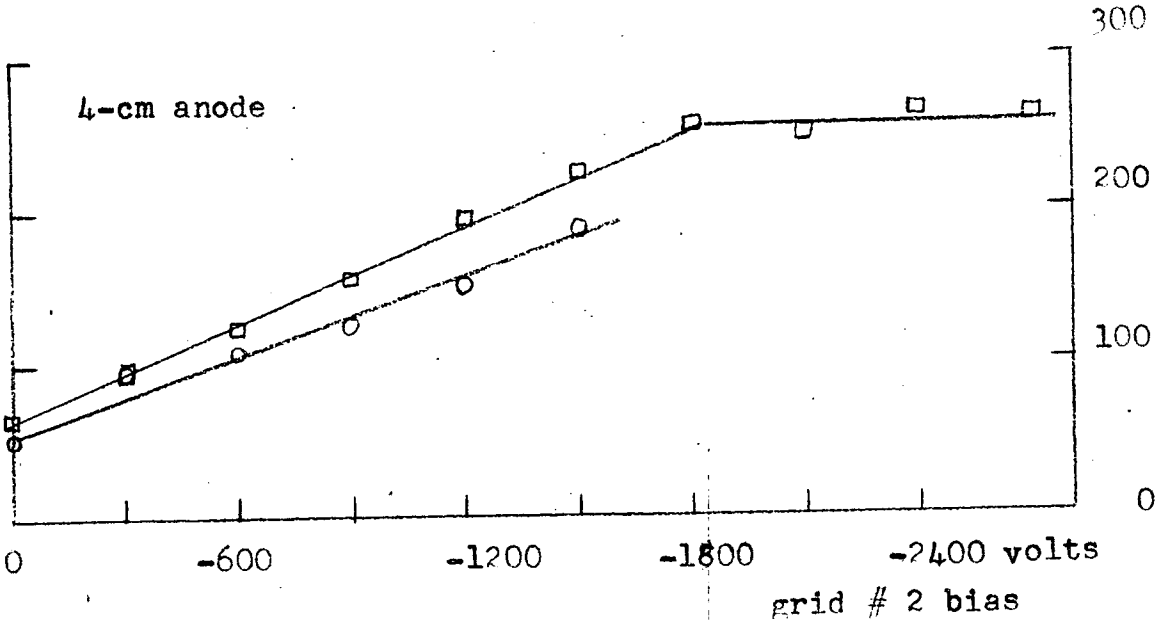

FIGURE 15

EFFECT OF CHARGING CURRENT ON LIMITING VOLTAGE

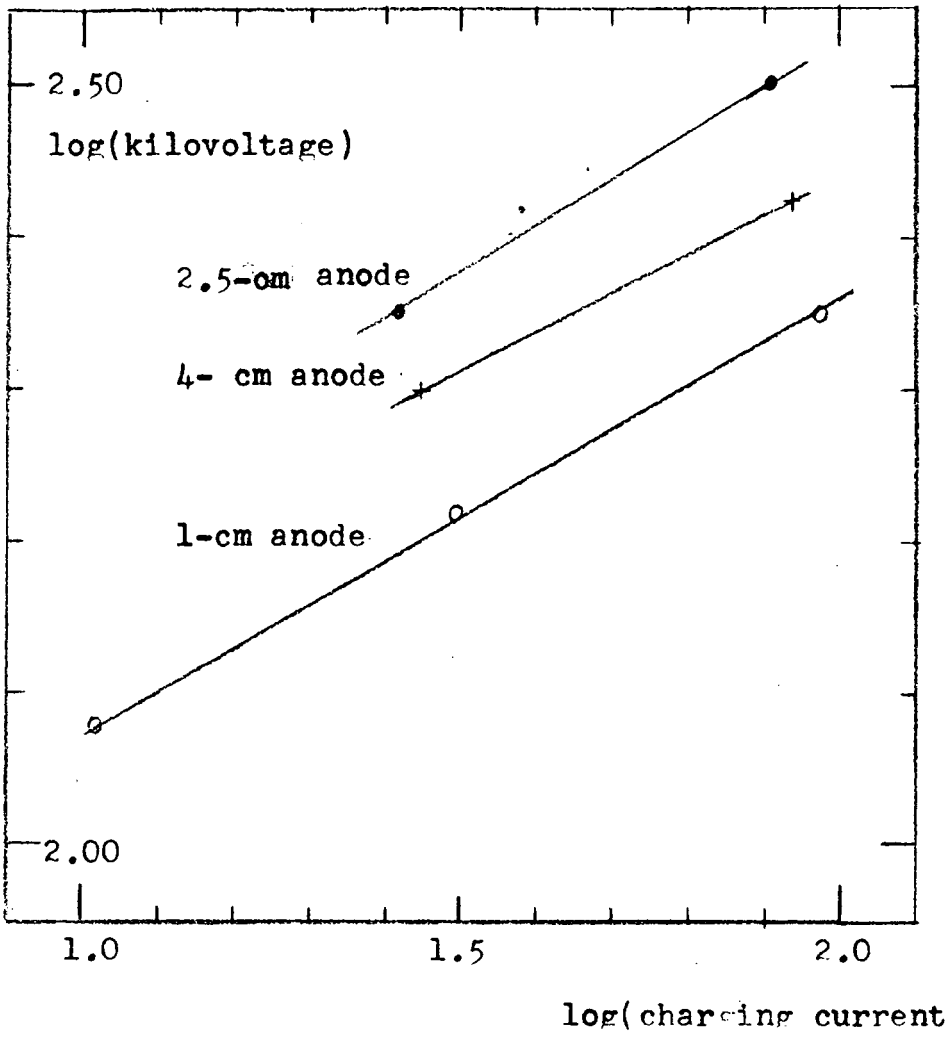

biased negatively with respect to the cathode, ordinarily draw currents at the limiting anode voltage. The magnitude of these currents varies with grid bias, anode voltage, charging current, and anode size.

Currents are also drawn by the grids during the period of time required for the anode to reach a limiting voltage. Figures 16 through 22 illustrate the changes in grid currents and anode voltage during this period for the various anodes. The source strength (charging current at zero volts) was 50 micromicroamperes in all cases. The quartz rod used with the 1-cm anode had an umbrella-like projection just below the anode.

The magnitude of the current flowing to grid 1, when the anode is 1 cm in diameter and grid 2 is biased negatively at -900 volts or more, varies approximately as the third power of the anode voltage. In figure 23 the log of grid 1 current is plotted against the log of anode voltage. Three source strengths are represented, 15, 50, and 180 micromicroamperes. In each case the bias on grid 2 was -1200 volts and the bias on grid 1 was 300 volts. Increases in the bias on grid 2 did not affect the current drawn by grid 1 under these conditions.

The relation of grid 1 current to anode voltage at high grid 2 bias is somewhat different for the 2.5 and 4-cm anodes. A plot of current against the cube of the voltage is not a straight line. In the case of the 2.5-cm anode the line is straight up to about 200 kilovolts. In the case of the 4-cm anode it is straight up to about 170 kilovolts. At voltages

FIGURE 16

1 - CM ANODE

Grid #1 , 300 volts ; Grid #2, -300 volts

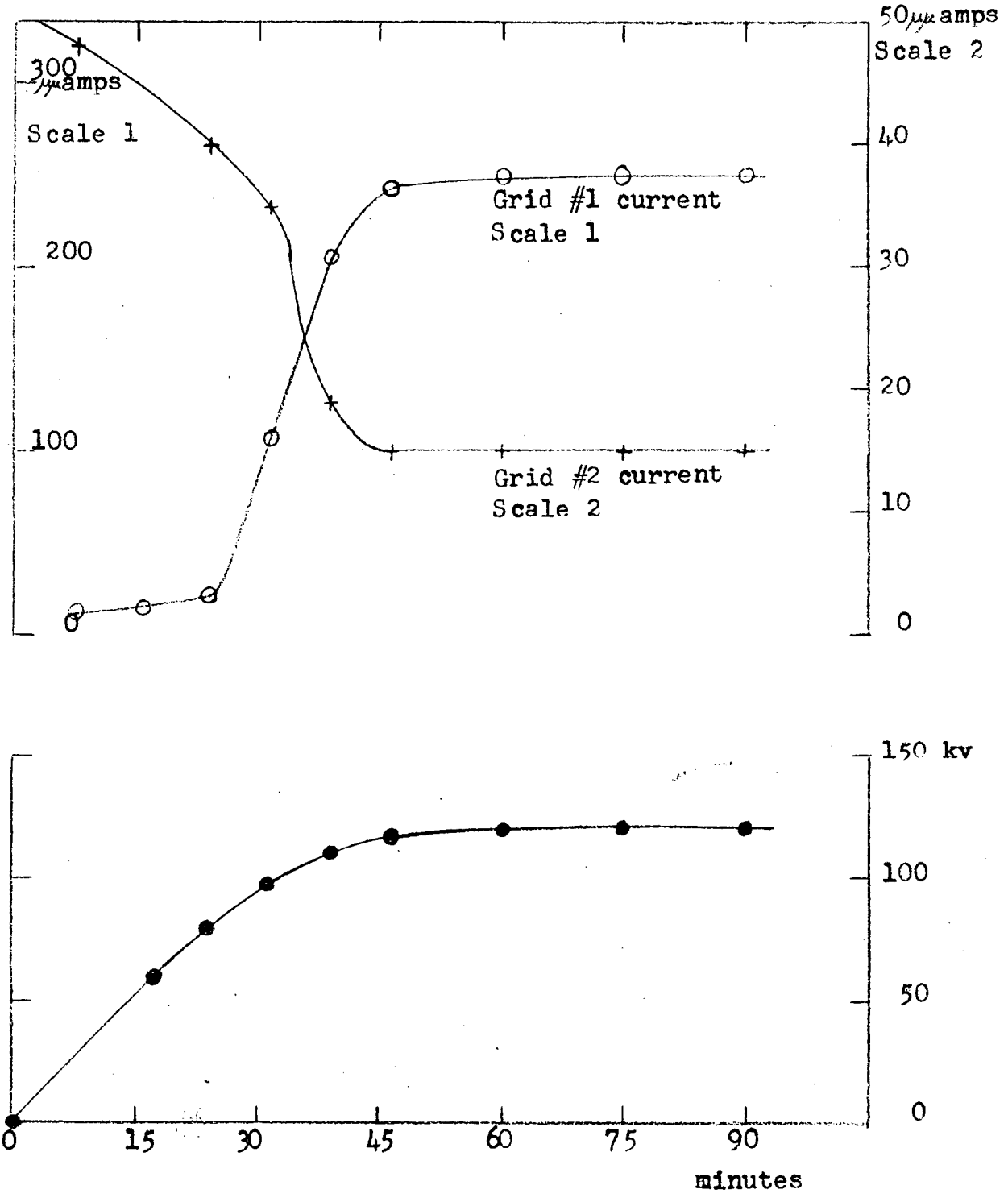

1 - CM ANODE

Grid #1, 300 volts ; Grid #2,-1800 volts

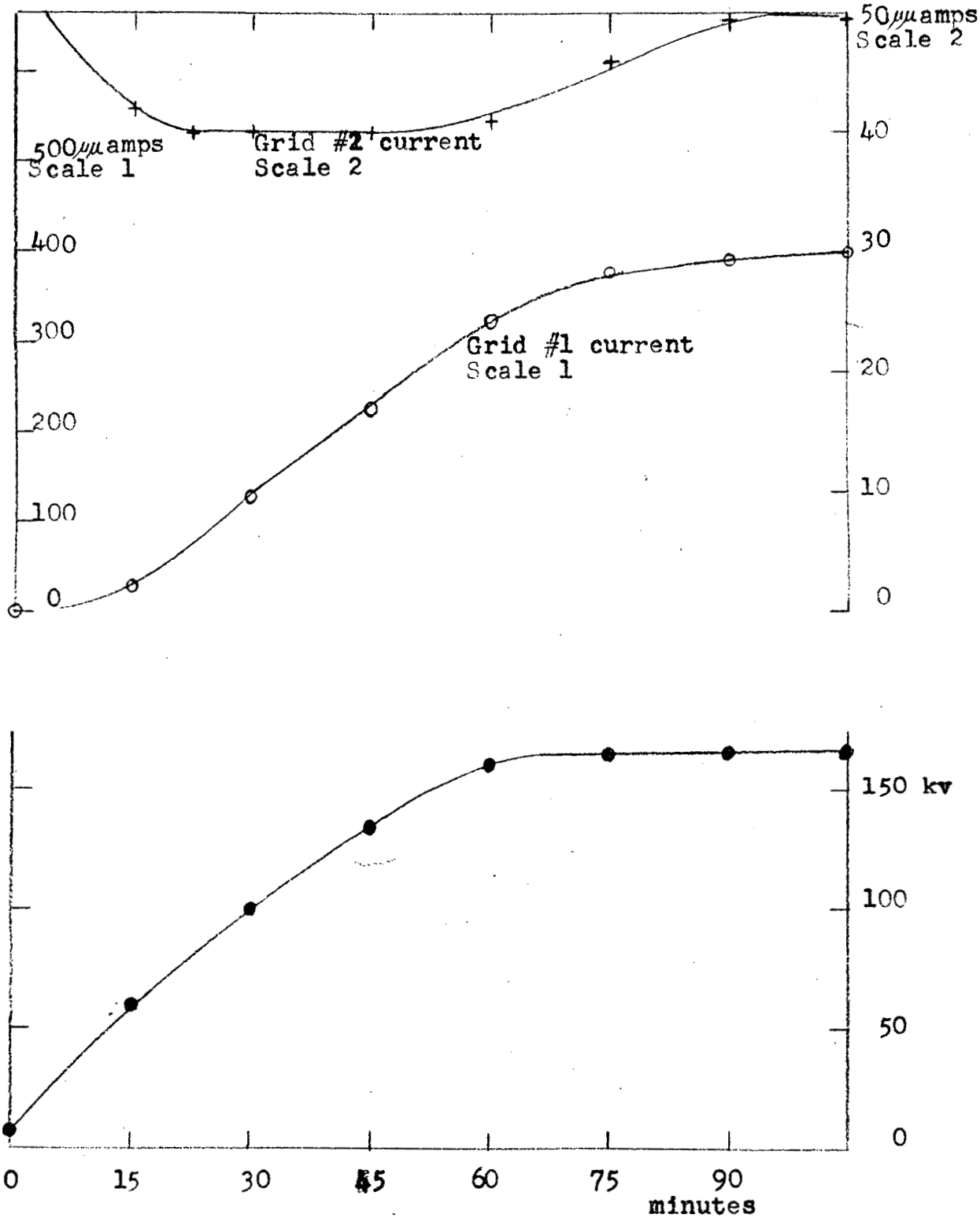

FIGURE 17

2.5- CM ANODE

Grid #1, 300 volts ; Grid #2, -600 volts

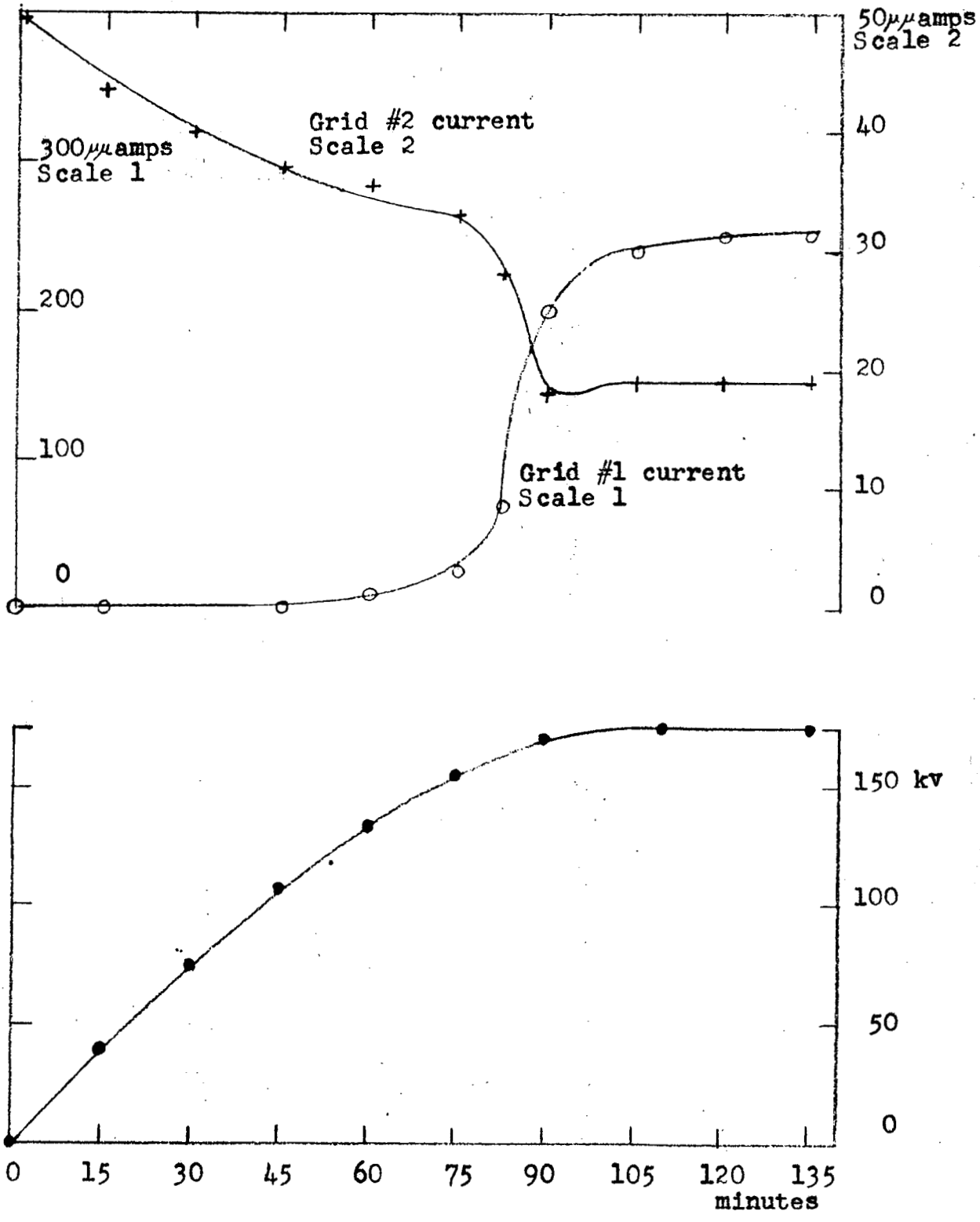

FIGURE 18

2.5- CM ANODE

Grid #1, 300 volts ; Grid #2 , - 1500 volts

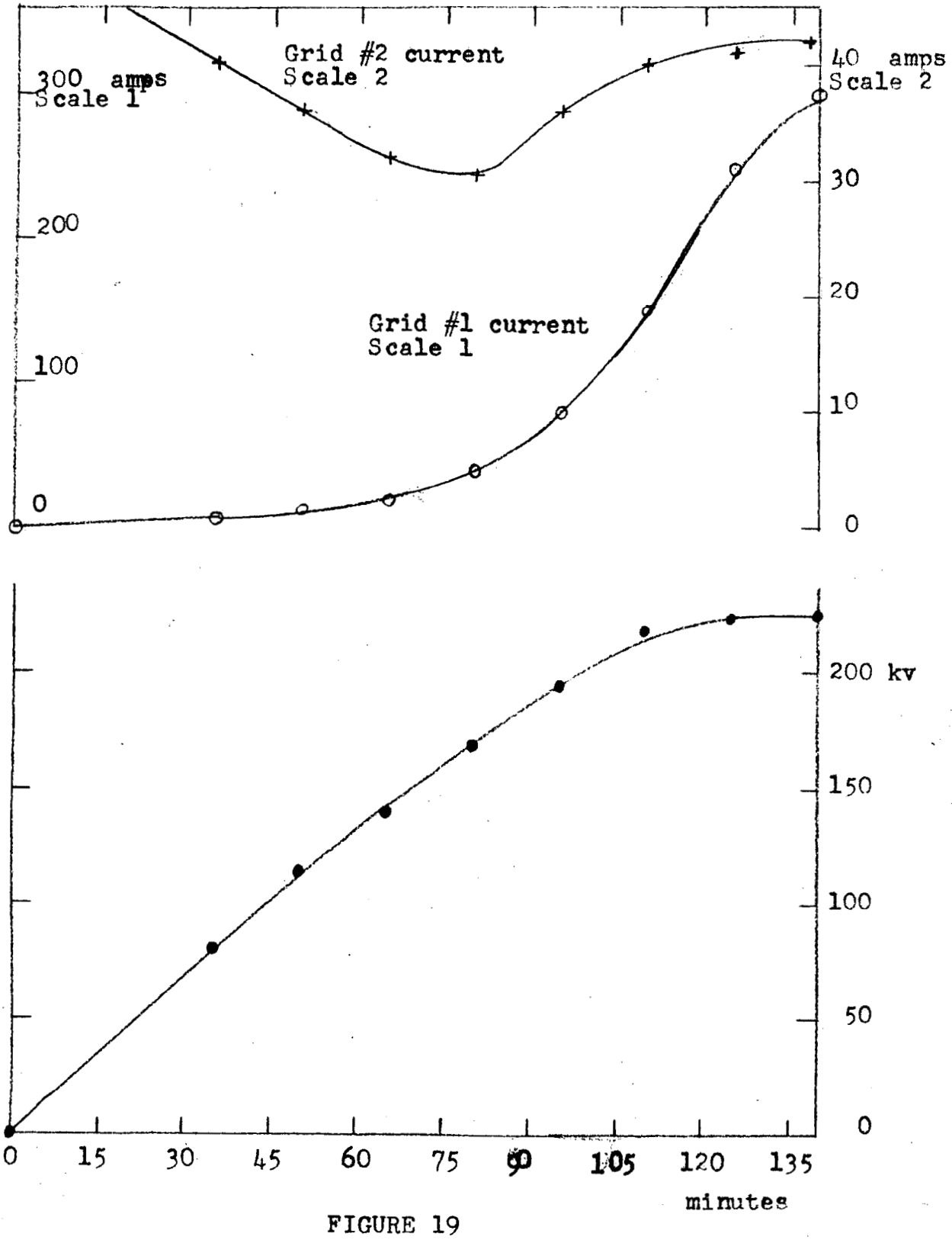

FIGURE 19

FIGURE 20

4 - CM ANODE

Grid #1, 300 volts ; Grid #2 , - 600 volts

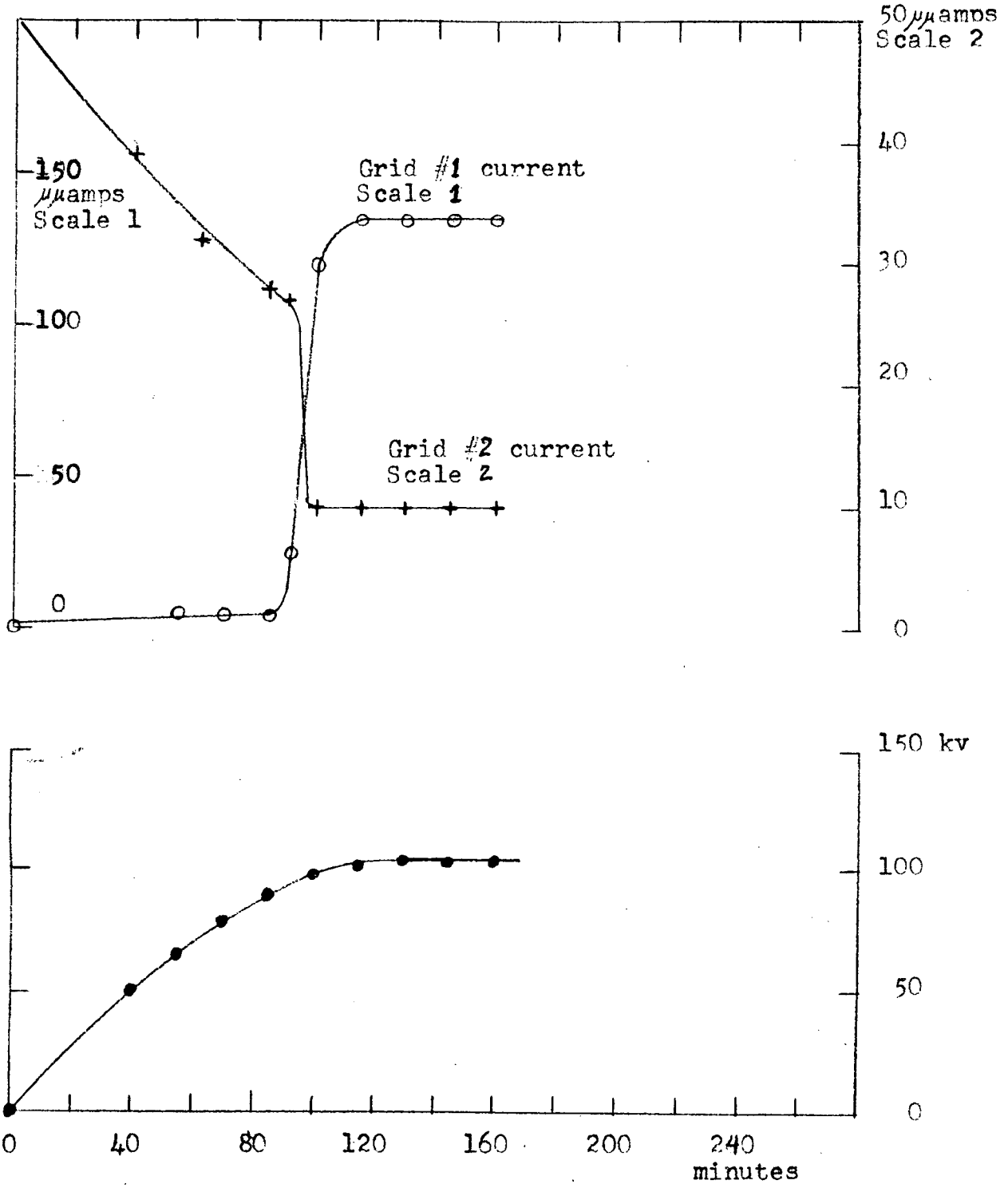

FIGURE 21

4 - CM ANODE

Grid #1, 300 volts ; Grid #2, -1200 volts

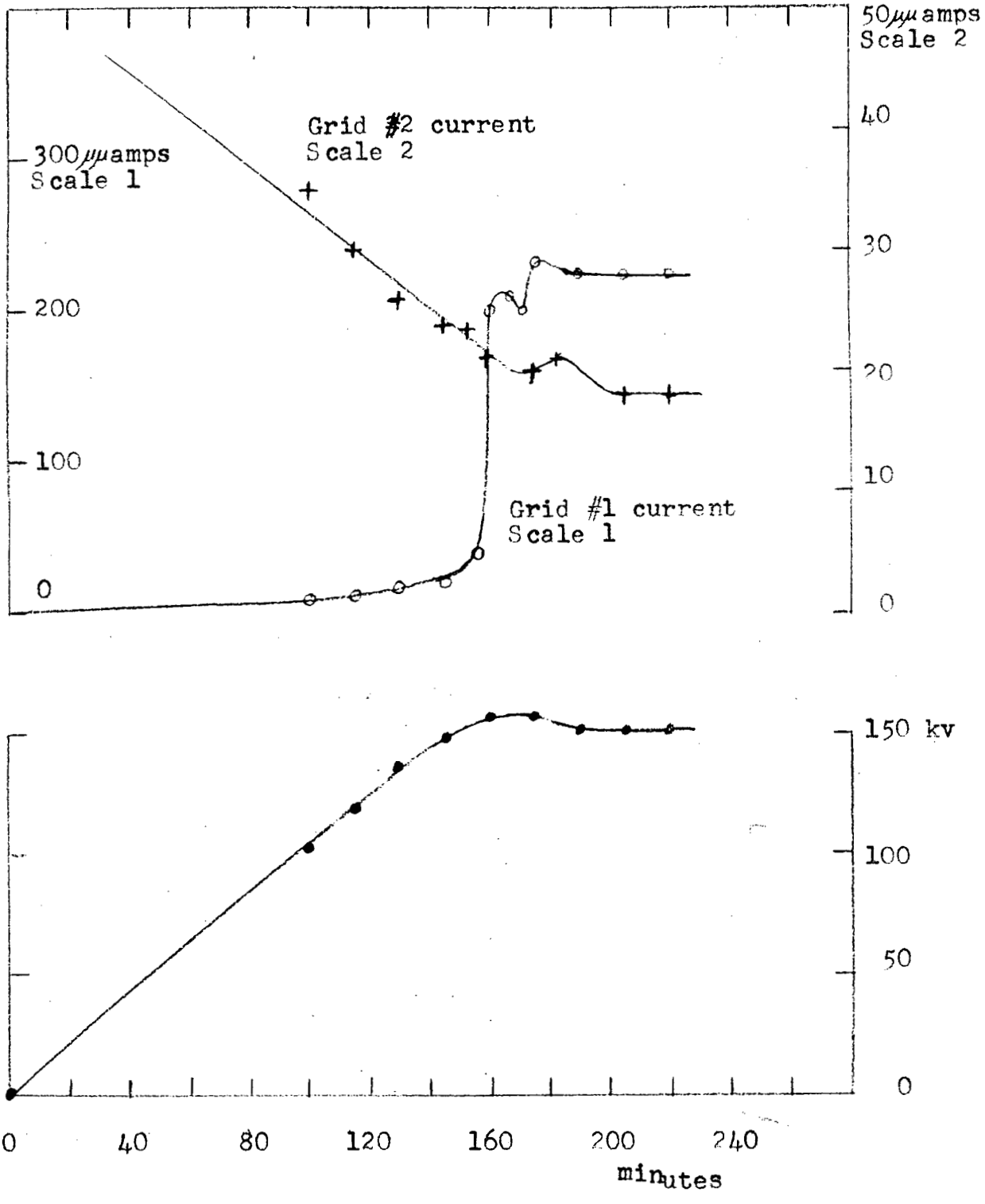

FIGURE 22

4 - CM ANODE

Grid #1, 300 volts ; Grid #2 , -1500 volts

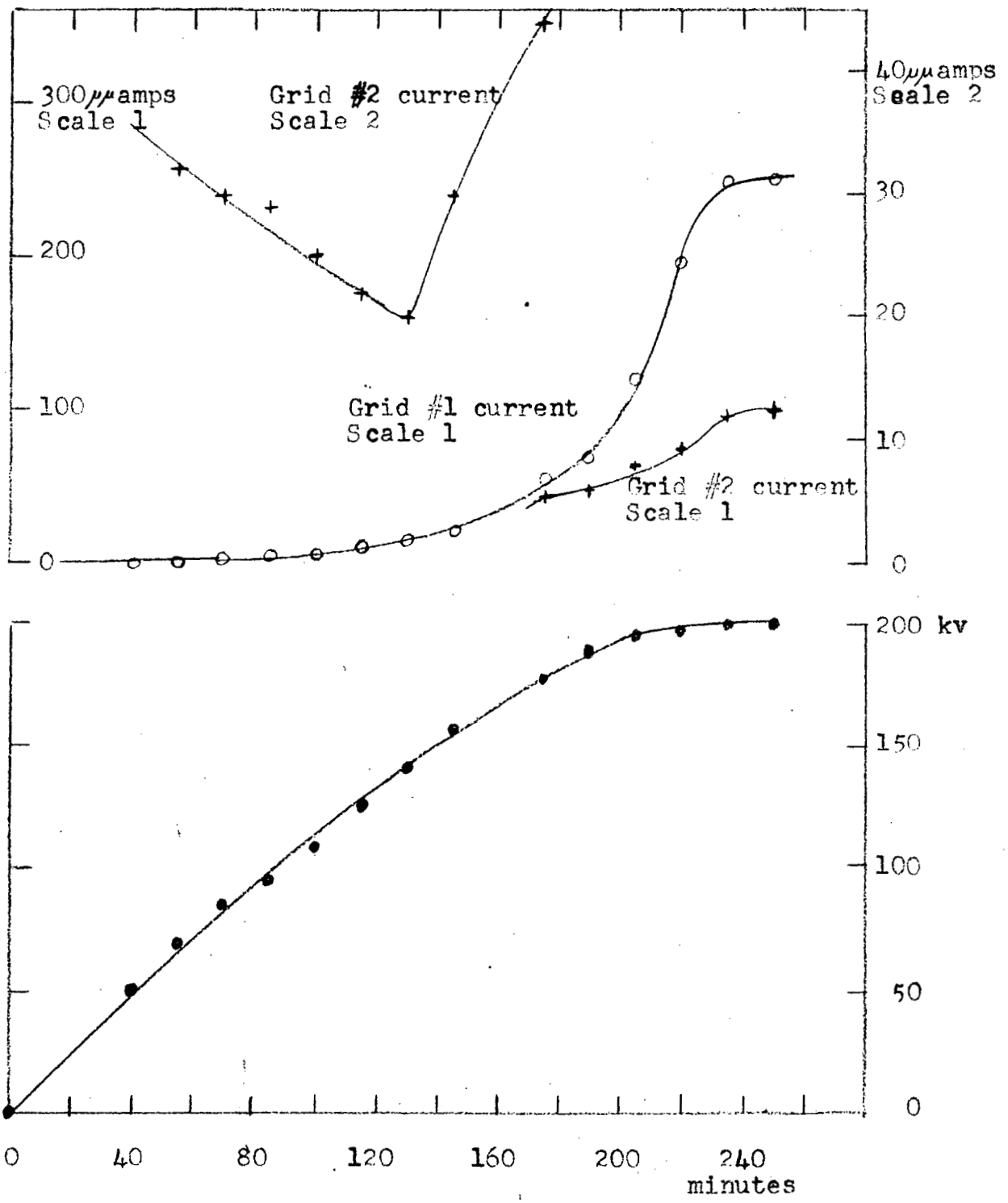

FIGURE 23

EFFECT OF ANODE VOLTAGE ON GRID - 1

CURRENT AT HIGH GRID - 2 BIAS

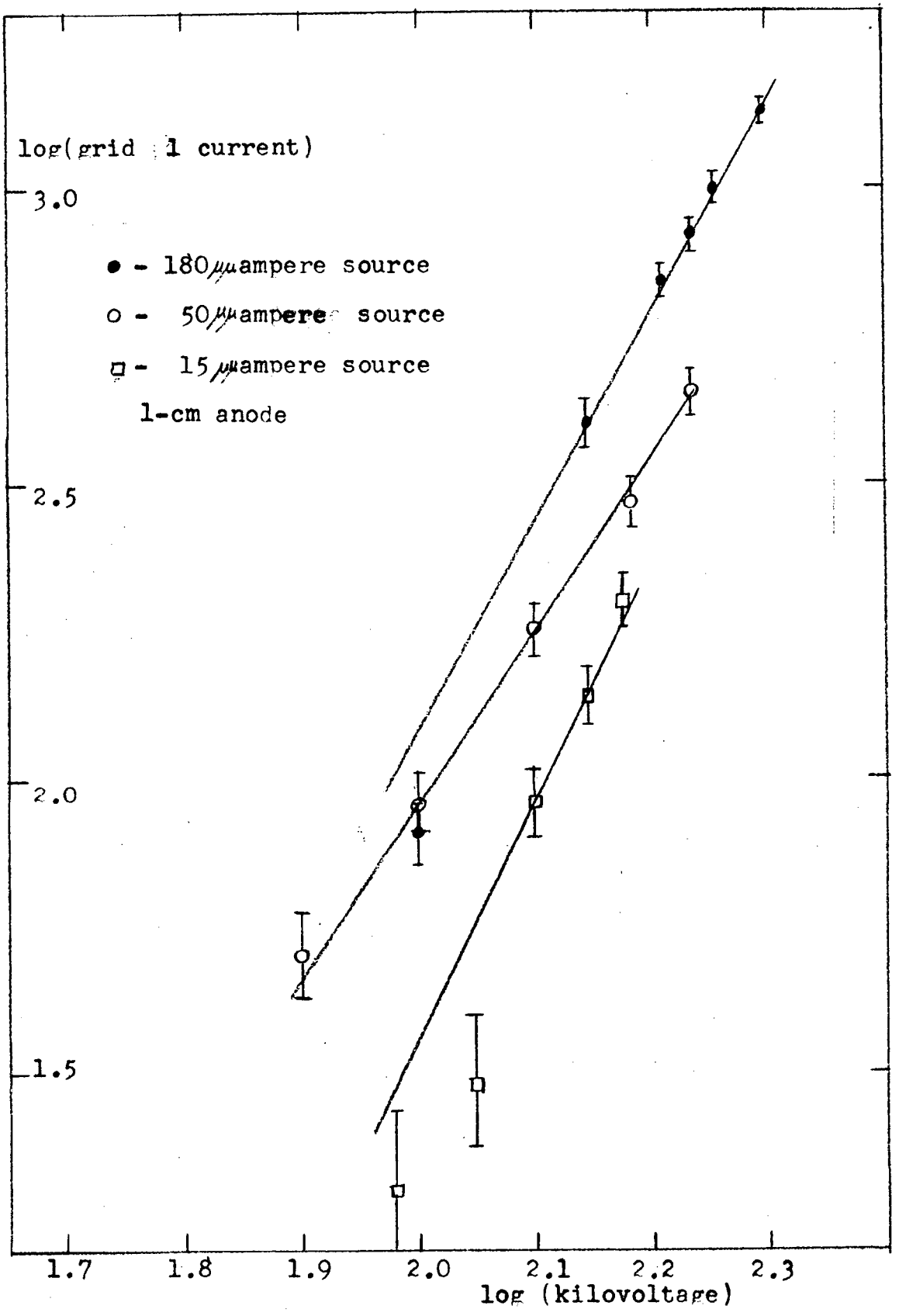

above these points the current increases more rapidly than the third power of anode voltage. This behavior is illustrated in figure 24.

When grid 2 is biased at a high negative voltage the current drawn by grid 1 is approximately proportional to the square root of the source strength. This is true of the 1-cm anode at all voltages. In the case of the 2.5 and 4-cm anodes this is true up to about 200 and 170 kilovolts respectively. Figure 25 illustrates this relation.

With all three anodes there is a "critical" grid bias beyond which increases in bias produce no change in voltage. (See figure 14.) At grid biases below this critical value the current drawn by grid 1 rises very rapidly as the anode voltage approaches a limiting value. This behavior is illustrated in figures 26 and 27 for the 4-cm anode and the 50-micromicroampere source.

The magnitude of the current drawn by grid 1 is independent of the potential difference between grid 1 and the cathode if this difference is greater than about 90 volts. The current drawn by grid 1 when positively biased is positive, indicating collection of negative electricity from the vacuum space or loss of electricity of the opposite sign to the vacuum space.

If the bias on grid 1 is made negative the current flow is in the opposite sense, indicating loss of negative electricity or collection of positive electricity. In one case with -1200 volts on grid 2 the current to grid 1 was 50 micromicroamperes

FIGURE 24

GRID -1 CURRENTS

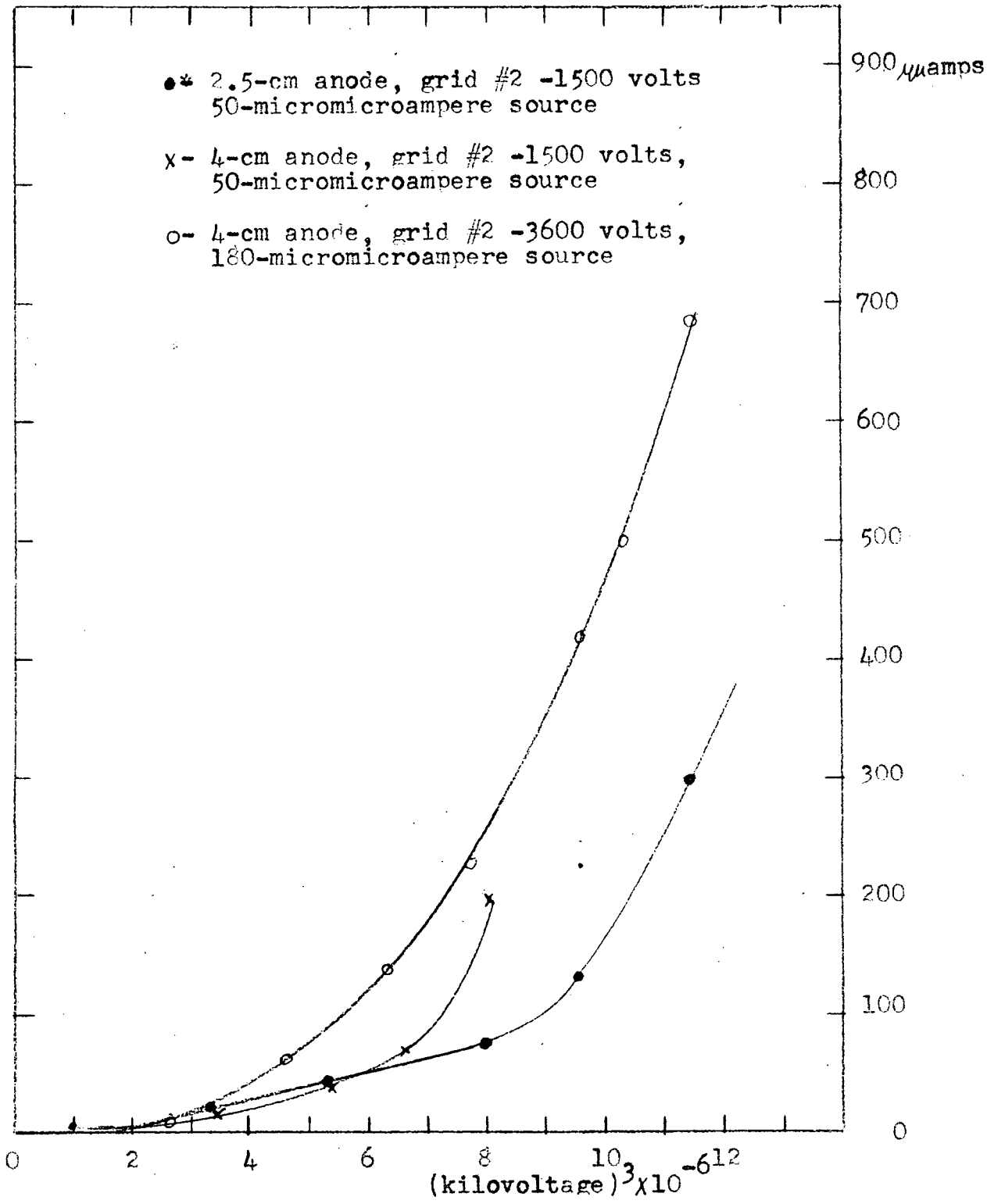

FIGURE 25

EFFECT OF SOURCE STRENGTH ON

GRID - 1 CURRENT

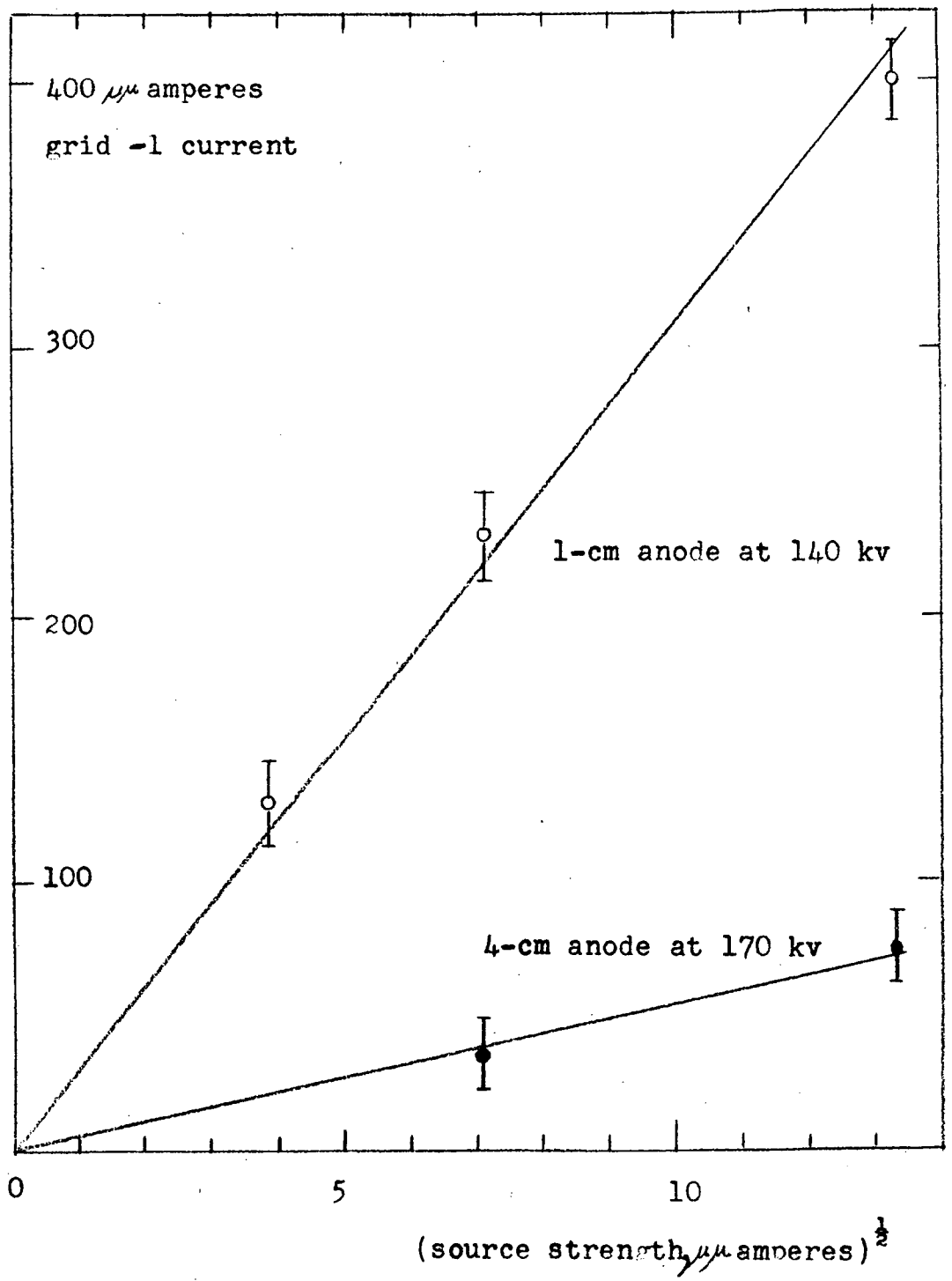

FIGURE 26

GRID -1 CURRENT WITH THE 4-CM ANODE AND VARIOUS BIASES ON GRID 2

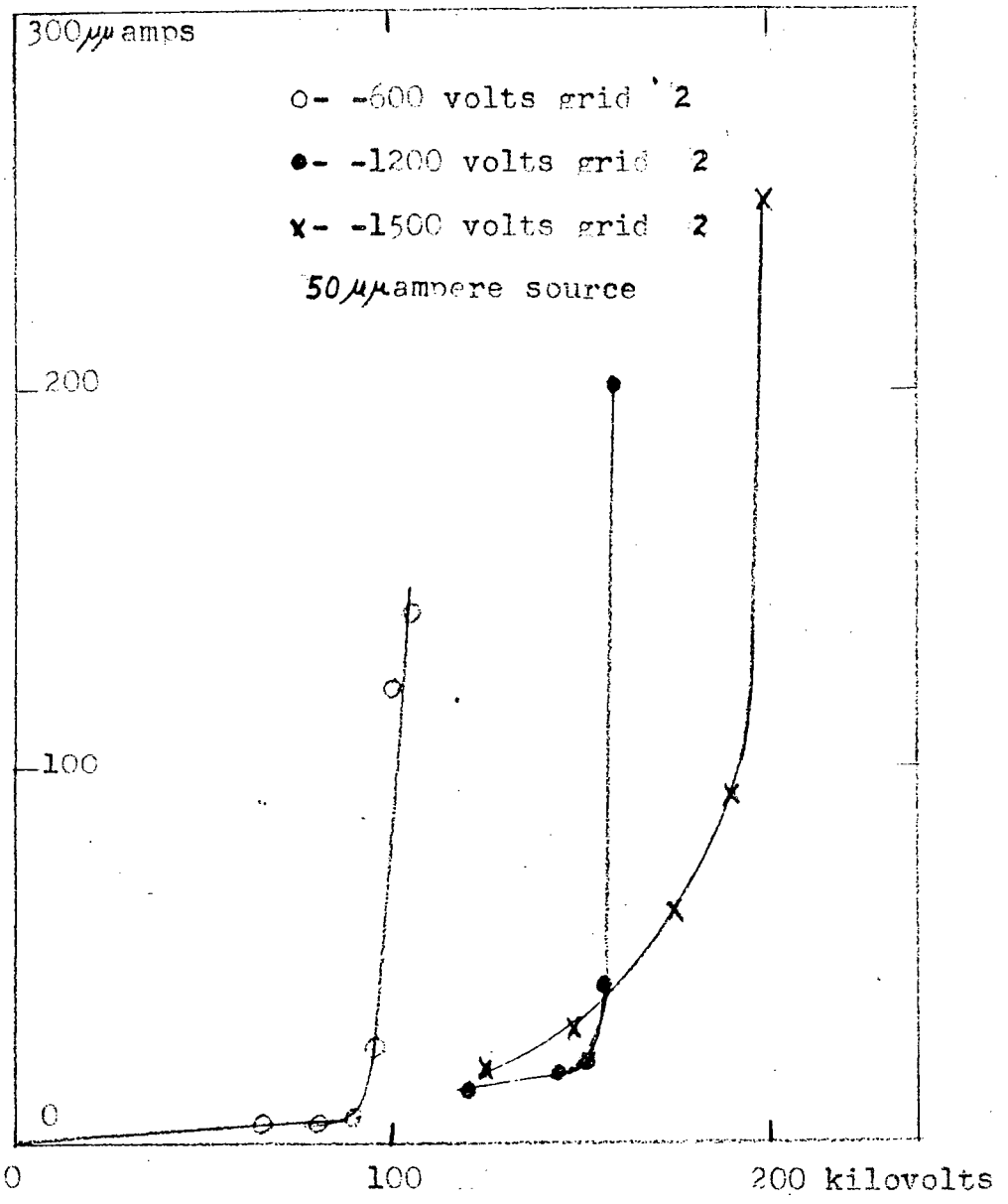

FIGURE 27

EFFECT OF ANODE VOLTAGE ON GRID # 1

CURRENT AT A LOW GRID # 2 BIAS

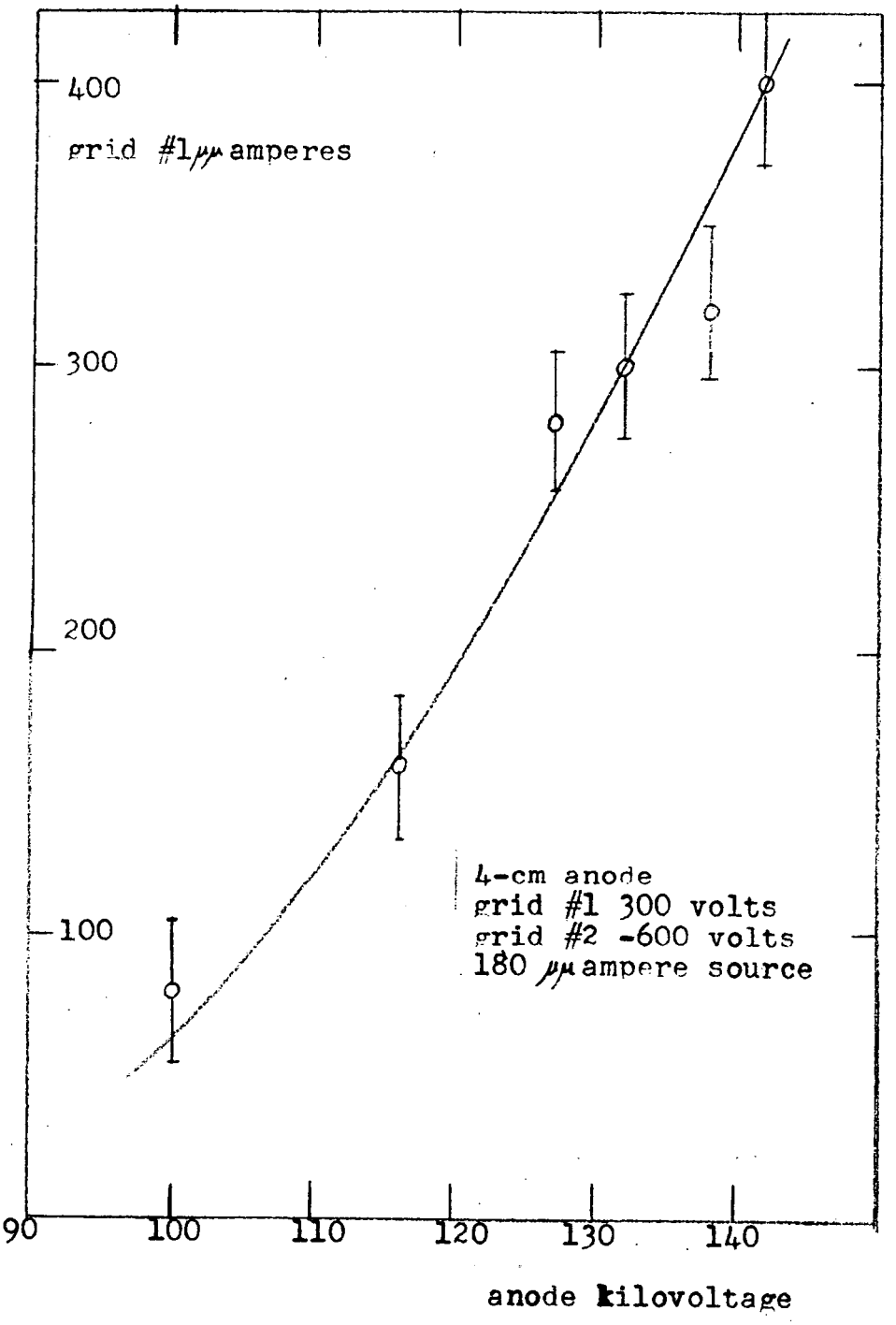

at -300 volts bias and 100 micromicroamperes at -600 volts bias.

As can be seen in figures 16 through 22 the current flowing to grid 2 is not a simple function of anode voltage or bias. The following features are observed. With zero anode voltage and the anode charging freely, grid 2 draws a current approximately equal to the charging current. To the extent that the cathode wall is cut off from the anode field by the grid bias, the grid is acting as the cathode and must increase its negative charge at the same rate that the anode positive charge increases. The grid obtains this charge by drawing a current from the external connection. As the voltage on the anode increases the charging current decreases, and correspondingly the current to the grid decreases. When the bias on grid 2 is below the critical value, the current to grid 2 drops sharply as the anode reaches the limiting voltage. In this condition there remains an appreciable grid-2 current due to collection of positive electricity or to loss of negative electricity by grid 2.

Measurements of the current flowing to two separate portions of grid 2 showed that the effects just discussed are evenly distributed about the axis of the chamber. Measurements made with separate top sections of both grids indicated that the effects were not spherically isotropic. The top section of grid 1 subtends approximately 0.04 of the total solid angle about the anode, but this section of the grid picks up from 10 to 20 per cent of the total grid 1 current at limiting voltage. Other evidence of anisotropy, especially with the

1-cm anode, will be presented later.

General observations

The baffle (b, figure 1) was ordinarily cooled with tap water. In one experiment ice water was pumped through the coils in sufficient quantity to maintain the temperature at about 7° C. In the course of several hours the anode voltage increased 15 kilovolts. When tap water was again passed through the coils the anode voltage dropped to its original value in about 30 minutes.

In one series of experiments two sections of grid 2 were biased at different voltages. The anode voltage obtained under these conditions was higher than that obtained with both grid sections at the lower bias but not as high as the voltage obtained with both grid sections at the higher bias.

Occasionally the quartz rod used to support the anode became unusable, presumably because of surface contamination. This condition was usually accompanied by spark discharge limitation of the anode voltage. However, in one instance, limitation of the voltage on the 4-cm anode was traced to a steady leakage of current from the surface of the rod. In this case the voltage was limited at 25 kilovolts, and grid 1 collected a negative current ten times the magnitude of the charging current.

Spark discharges

At times the anode voltage was limited by spark discharges. Discharges sometimes occurred after the anode voltage had leveled off at a dark-current-limited value. These discharges

can be grouped in two categories. The first category includes discharges in which the anode charge is almost completely neutralized. The second category includes those discharges in which the anode voltage is reduced by about 20 kilovolts or less.

The first type of discharge is accompanied by large bursts of current to all sections of both grids. The coulomb content of the current collected from the vacuum space by grid 2 during one of these discharges was usually several times the anode charge at the initial voltage and was invariably positive. A simple exchange of charge between the anode and grid 2 would not produce a flow of current from an external source. Thus the fact that grid 2 did draw a current indicates that more charged particles entered the vacuum space during a discharge than were required to neutralize the anode charge. During one of these discharges grid 1 collected from the vacuum space an amount of negative electricity equivalent to something between 10 and 20 times the charge on the anode.

Discharges of a few to about 20 kilovolts were variable in their effect on grid currents. In one instance a negative pulse was observed on one section of grid 2, and a positive pulse was observed on the other section of grid 2. A positive pulse appeared on grid 1. This behavior indicates that these small discharges are sometimes anisotropic about the anode. Variations in this behavior included the appearance of negative or positive pulses on all of grid 2. Occasionally one section of grid 2 collected just the appropriate charge to offset the

drop in anode voltage and no pulse appeared on that section.

The charges collected by the grids as a result of a discharge were not collected instantaneously. The voltage drop across a resistor rose very rapidly to a maximum and then decayed approximately exponentially with a half time of about a minute. The RC time of the circuit during these observations was much less than a minute.

These two types of spark discharges were encountered with all three anode sizes and with most grid biases. With the 2.5 and 4-cm anodes and with the grids at ground potential the discharges were almost exclusivly in the first category. In one experiment a 2.5-cm teflon anode was limited by discharges of the second type.

The tendency to spark discharge decreases markedly as the anode size increases. The probability of discharge with the 1-cm anode was so great that it was often difficult to maintain a steady high voltage. The opposite was true with the 4-cm anode; with it spark discharge was usually rare. When the bias on grid 2 was suddenly reduced to zero volts, the voltage on the 4-cm anode decreased rapidly, usually in a matter of less than a second, to the limiting voltage for zero grid bias. Similar experiments with the 1-cm anode usually produced a spark discharge to zero kilovolts. A quartz umbrella-like projection on the supporting rod reduced the tendency of the 1-cm anode to be limited by spark discharge but did not increase the limiting voltage appreciably.

Pressure effect

The behavior of the system was found to be approximately independent of residual gas pressure for pressures below about 10^{-4} mm Hg. When the pressure was allowed to rise above this value, small increases in anode voltage were usually observed. At about 10^{-3} mm Hg the gas induced a discharge. Results of a typical experiment are illustrated in figure 28.

Positive ions

The electron multiplier described in section II of this thesis was used to detect energetic particles originating at the anode surface. In the following paragraphs we present some general observations with regard to these particles. Later we will describe their composition and specific effects in more detail.

Early experiments with the positive ion counter showed that at every steady limiting voltage a number of energetic particles were being emitted from the surface of the anode. A typical pulse height spectrum obtained with the electron multiplier is illustrated in figure 29.

Electric deflection of these particles showed that the majority of the particles were positively charged. A potential difference of a few hundred volts between two parallel plates (see figure 12) served as a means of deflection. When a beam of charged particles traverses an electric field perpendicular to the line of flight of particles, the beam is deflected an amount proportional to the intensity of the field and inversely proportional to the energy per unit charge of the particles.

FIGURE 28

PRESSURE EFFECTS

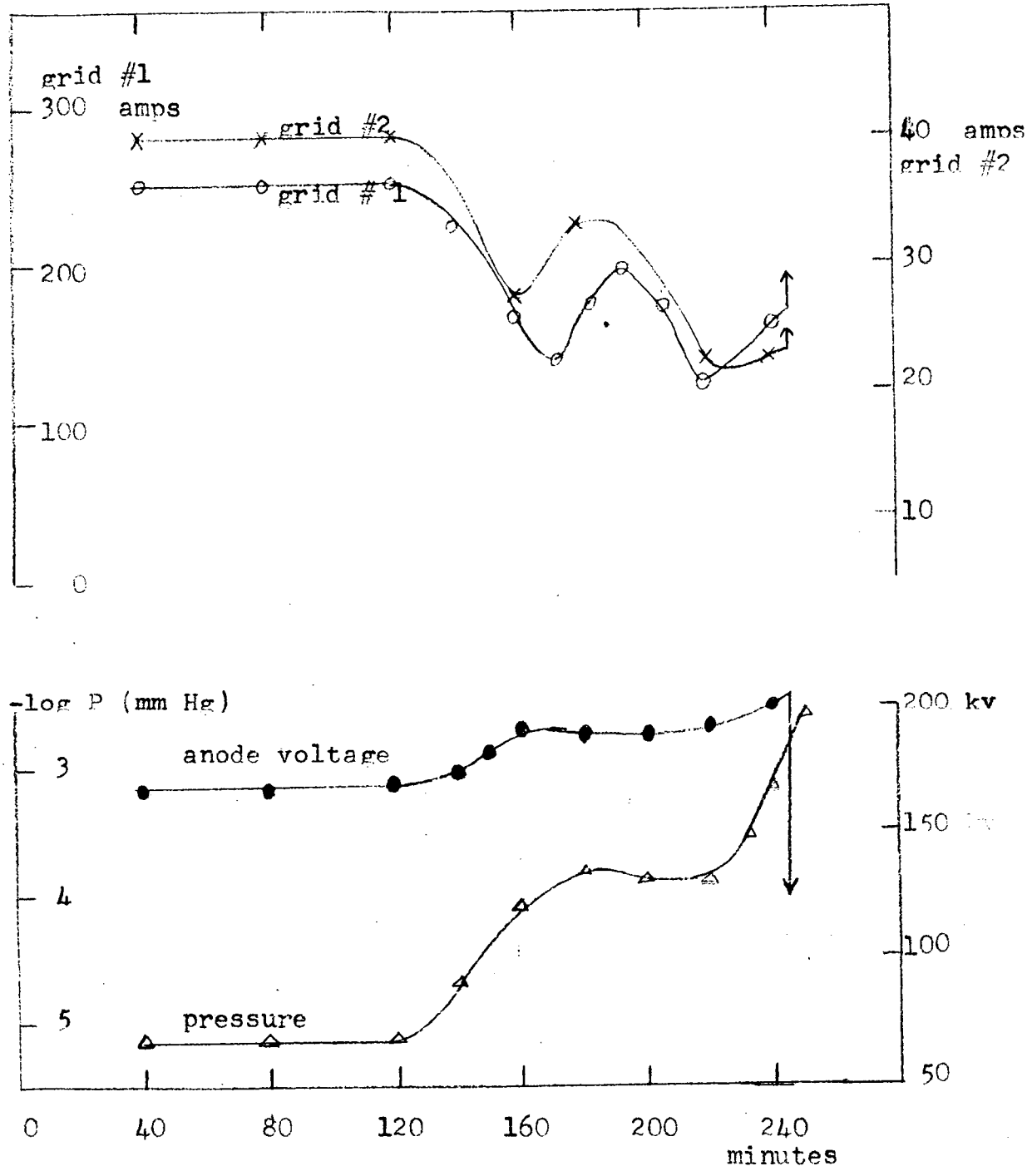

FIGURE 29

PULSE HEIGHT SPECTRUM

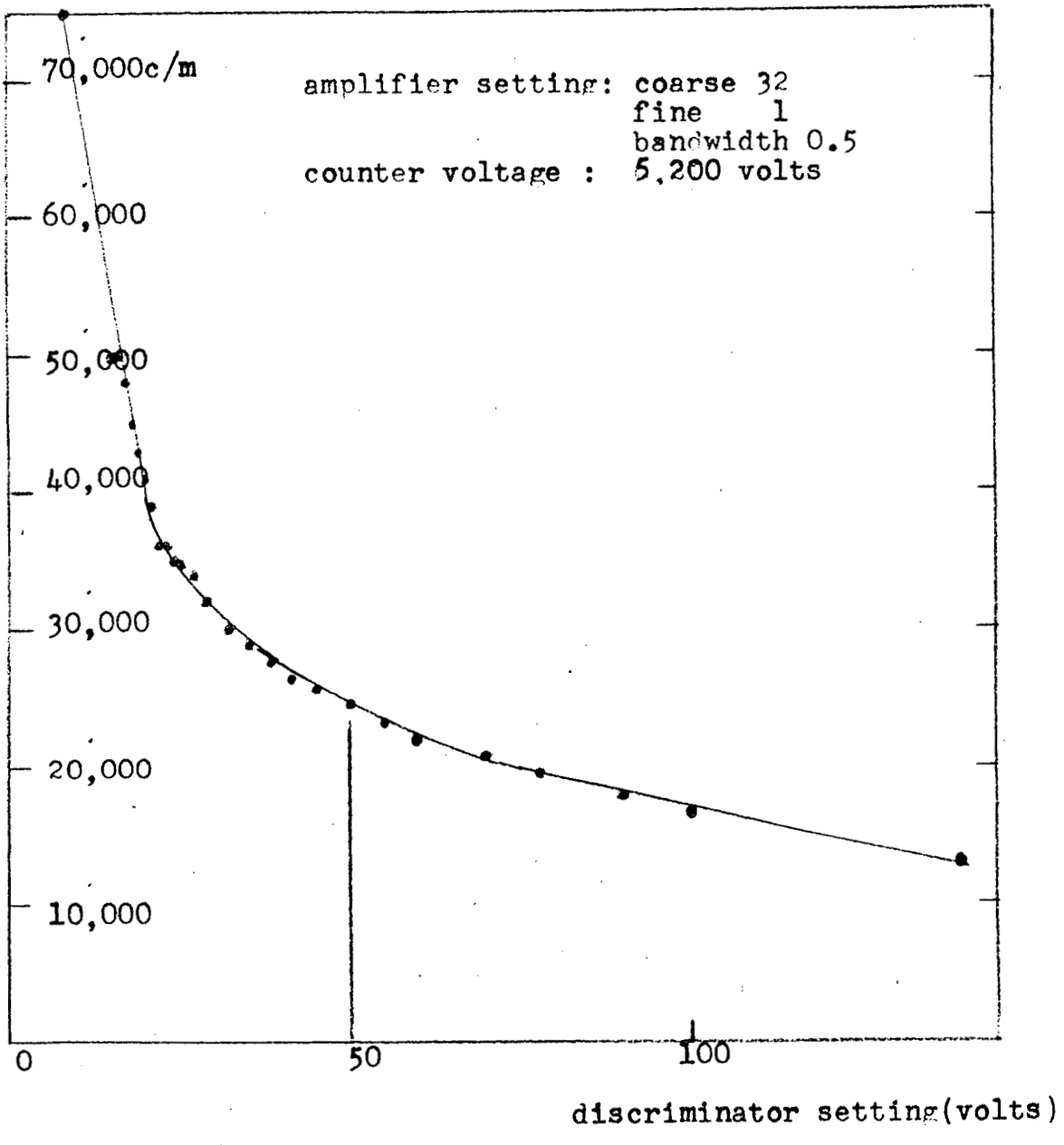

Figure 30 illustrates a typical result of such an experiment in our system. The large peak at the left represents the total beam of particles with no deflecting field. The curve following the solid dots represents the spectrum with an electric field of 800 volts cm^{-1} across 10 centimeters of the path of the beam. The major portion of the beam was deflected 0.71 inch in the direction of the negatively charged plate. About 7 per cent of the total beam was not deflected by the electric field. We interpret this to mean that about 7 per cent of the positively charged particles decompose into a neutral and a charged fragment at some point in the path between anode and deflection plates. The tail on the right side of the deflected peak was reproducible and apparently represents particles with slightly less than the maximum energy per unit charge.

The accelerating voltage through which the positively charged particles had passed was calculated from the magnitude of the deflection. In every case this voltage corresponded with the anode voltage; in fact, as was mentioned previously, this method was used as an independent check on the anode voltage.

The height of the undeflectable "neutral" peak relative to the height of the total positive ion peak varied from about 3 to about 20 per cent. This variation did not appear to be related to anode size or voltage or to the grid bias.

In early experiments two peaks were observed with no deflecting field. This phenomenon occurred only when the 1-cm anode was used with the umbrella-rod. The peaks were separated

FIGURE 30

ELECTRIC FIELD DEFLECTION OF POSITIVE IONS

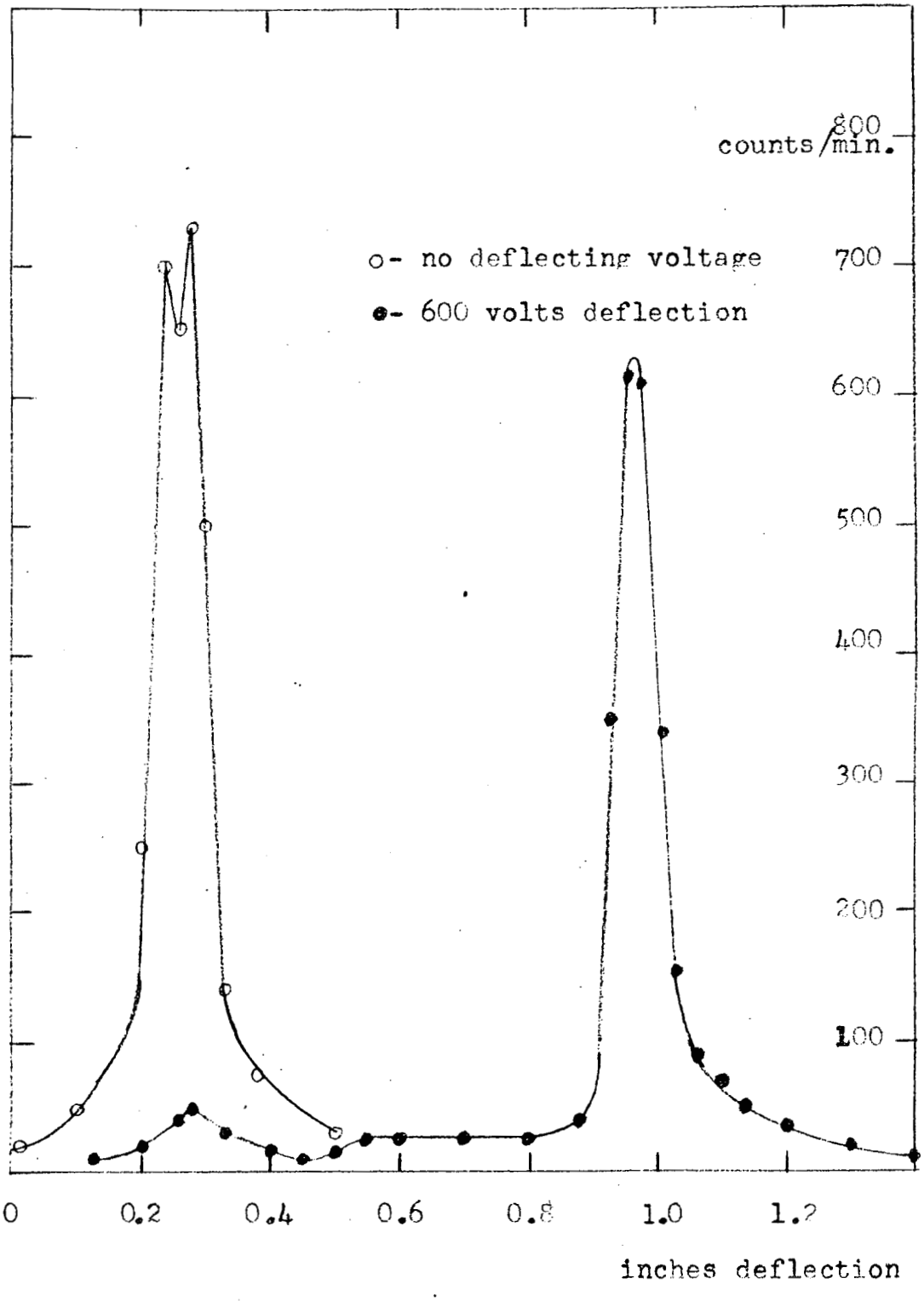

by a distance which corresponded with the distance between the center of the anode and the upper edge of the umbrella-like projection on the rod. Electric deflection of the two peaks indicated that they had been accelerated through voltages which differed by no more than about 40 kilovolts. The height of the peak due to particles from the umbrella was extremely erratic, varying in a few minutes from about the same magnitude as the peak due to particles from the anode to about one-tenth that value. Because of this erratic behavior, quantitative data were not obtained as to accelerating voltage or mass-to-charge ratios for the particles originating at the umbrella.

In later experiments, this peak from the umbrella was excluded by defining a narrow path from the anode to the counter. The charge on the umbrella was still apparent from another phenomenon. With the 1-cm anode supported on the umbrella-rod, the position of the beam at the counter shifted slowly upward as the anode voltage increased. This would result if the voltage on the umbrella were always a fixed number of kilovolts below the voltage on the anode. Thus as the anode voltage increased, the distortion of the field surrounding the anode would increase. Under the same circumstances it was noted that the position of the neutral peak differed from the position of the positive ion peak when no deflecting field was applied. The positions of these two peaks were such that the neutral particles apparently originated at a point about 0.1 mm above the point of origin of the positive ions. This is an indication that the fragmentation which resulted in the formation of most

of the neutral particles took place close to the surface of the anode.

The counting rate of the positive ions is in general a function of the anode voltage. Figure 31 illustrates this dependence for the 1-cm anode with grid 2 at -1200 volts and grid 1 at +300 volts. The current drawn by grid 1 is included for purposes of comparison. The source strength was 180 micromicroamperes. This curve is typical of the 1-cm anode for all grid-2 biases above the critical value. A similar relation between the counting rate and grid-1 current is found for the 2.5 and 4-cm anodes. (See figures 18-22, 31, 32.)

Counting rate versus voltage curves at low grid-2 biases are illustrated for the 2.5-cm anode with a 50-micromicroampere source in figure 32. Similar results are obtained with the other anodes.

The counting rate at a limiting voltage was found to vary with the voltage. Table 3 illustrates this dependence for the three anodes. These numbers were obtained with a 180-micromicroampere source. The slit limiting the number of particles which can strike the counter subtended 6.4×10^{-6} of the total solid angle about the anode and was in the equatorial plane of the anode. The values for the 1-cm anode were obtained with an umbrella-rod; no provision was made to block off the particles coming from the umbrella.

FIGURE 31

EFFECT OF ANODE VOLTAGE ON

COUNT RATE WITH THE 1-CM ANODE

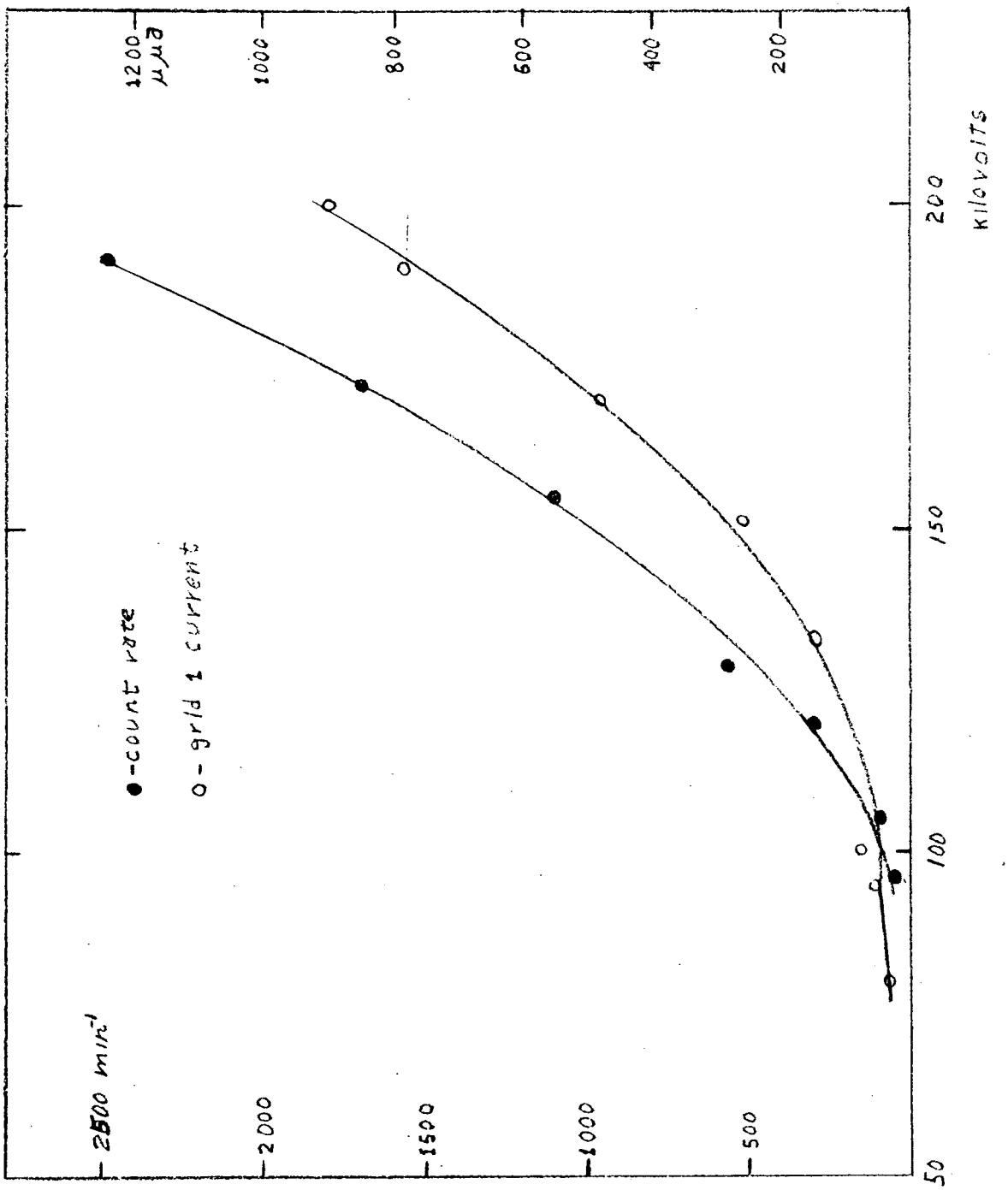

FIGURE 32 EFFECT OF VOLTAGE ON COUNT RATE

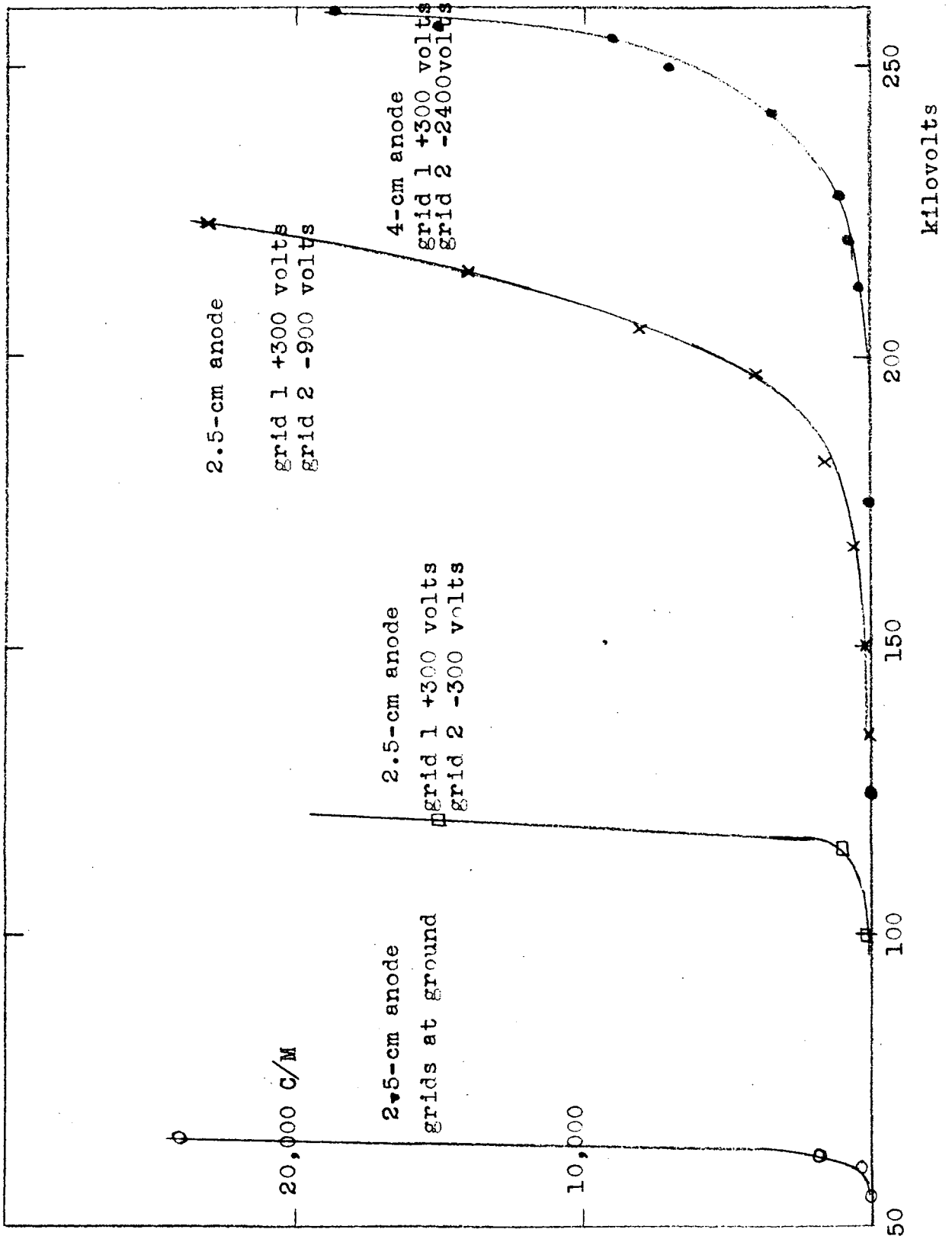

Table 3

Grid-2 bias	1-cm anode		2.5-cm anode		4-cm anode	
	anode voltage	count rate x 10^{-3}	anode voltage	count rate x 10^{-3}	anode voltage	count rate x 10^{-3}
grid removed					55 kv	4 min^{-1}
0 volts	80 kv	2.6 min^{-1}	80 kv	6 min^{-1}	65	13
-300	155	5.5				
-600			215	10	125	20
-900	220	13			155	33
-1200			310	15	195	40
-1800	225	23			250	46
-2400	225	23				

At times the counting rate was steady, at other times it was unsteady. In general the counting rate was steady at high limiting voltages with a high bias on grid 2 and unsteady with a low bias on grid 2. At low grid-2 biases the particles appeared in bursts ranging from about 1 to more than 60 milliseconds in duration. Each of these bursts produced from 10 to more than 1000 counts. The frequency of the bursts was such that successive 1-minute counts, at a counting rate of about 10,000 min^{-1}, differed by less than about 10 per cent. These bursts were observed to coincide with bursts of current to grid 1.

A considerable number of "double pulses" were observed in oscilloscopic obsevations of the pulses from the electron multiplier. These appeared much too frequently to be merely

accidental coincidences. The second of the two pulses usually appeared within about 3 microseconds of the first and was about half the magnitude of the first. Visual estimates indicated that something less than one in ten of the pulses appearing on the oscilloscope were double.

The immediate effect on the counting rate of a change of grid bias was found to depend on anode size and potential and on the initial grid bias. Changes in grid bias when both initial and final bias were above the critical value produced no effect on the counting rate. When the anode voltage was initially above the limiting voltage for the final grid bias a reduction in grid-2 bias produced a burst of particles. The 1-cm anode usually spark-discharged under these conditions; the 4-cm anode sometimes produced a high count rate for about a second which then leveled off at a lower voltage. When the anode was limited with a grid bias below the critical value, an increase in grid-2 bias produced a sharp reduction in counting rate. The count rate a few seconds after such an increase was the same as that normally obtained at that voltage with that grid bias. Increasing the bias on any one section of grid 2 was as effective in producing this effect as increasing the bias on all of the grid.

A few oscilloscopic observations were made with the 4-cm anode to determine the time required for the positive ion counting rate to decrease from a high value at a limiting voltage to a low value when the bias on grid 2 was suddenly increased. A SPDT switch was used to switch from a low bias to

a high bias. The sudden change in voltage on the external lead to grid 2 was used to trigger the sweep circuit of the oscilloscope. The output of the pulse amplifier was fed to the vertical input of the oscilloscope. When the grid voltage change occurred during a burst of counts, counts continued to appear at a high rate for lengths of time up to about 1 millisecond.

Positive ions in spark discharges saturated the counting circuit so observations of these were made with an oscilloscope. A composite pulse, presumably made up of a large number of individual pulses, appeared during every discharge. The pulses lasted about 1000 microseconds and were composed of two parts. An initial pulse lasted about 5 to 10 microseconds and was followed in about 100 microseconds by a much longer portion lasting about 1 millisecond. The heights of the two portions were not greatly different, each being about 20 times the height of a pulse obtained from a single particle. These observations were made with the 1-cm anode only.

Mass spectra

The mass spectrometer described in the experimental section was used to determine the mass-to-charge composition of the beam of positive ions originating at the anode surface. These mass-to-charge ratios were found to extend from less than 1 atomic weight unit per electronic charge to more than 2000. A typical spectrum is illustrated in figure 33.

The absolute accuracy of the mass-to-charge ratios is

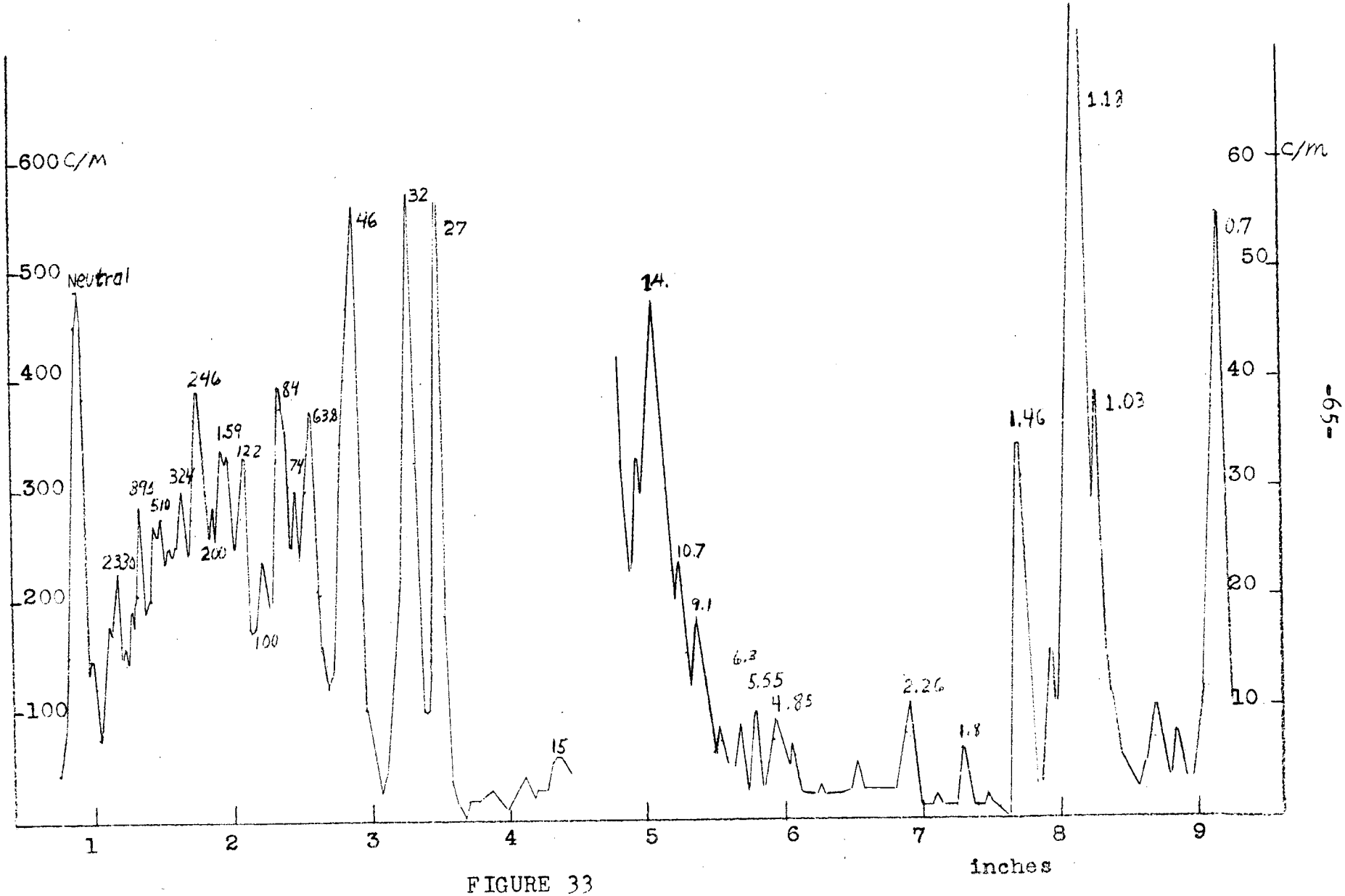

FIGURE 33

TYPICAL MASS SPECTRUM

probably no better than about ± 15 per cent. The magnets were calibrated by measuring the deflection of a beam of polonium-210 alpha particles. Two major sources of error were the variation of magnetic field with time and the uncertainties in anode voltage.

Attempts to discover significant trends in changes in the spectra as grid bias and anode size were varied were unsuccessful. Large variations in the relative intensities of the various peaks were observed from day to day even when attempts were made to keep conditions as constant as possible. The peak at mass 32 was found to be particularly subject to fluctuation.

Table 4 shows a list of mass-to-charge ratios of the particles and indications of the relative abundance of each species. The numbers represent average values obtained from seven spectra. In each case for mass-to-charge ratios of 13 and above, the peak close to 27 was taken to be 27, and all other numbers were normalized to this value. For mass-to-charge ratios below 13, the peak closest to 1.0 was chosen as 1.0, and other numbers were normalized to this value. Two normalization points were necessary because a single magnet could not be used satisfactorily for the entire spectrum. Actual values for the peak taken to be 27 ranged from 24.5 to 28; those for the peak taken to be 1.0 ranged from 1.08 to 1.20.

Table 4

Mass Charge	Relative intensity	Mass Charge	Relative intensity	Mass Charge	Relative intensity
0.65	13	27	105	160	70
1.0	35	32	105	215	35
1.4	13	45.7	100	244*	30
1.64	3.5	63.3	27	324*	43
2.0	4.4	73.5	44	425*	35
8.8	4.4	83	65	511*	
13	19	101	41	895*	43
14		121	52	1627*	30
15				2395*	30
				infinite	87

*These peaks were not always present.

Contamination of the anode with substances such as sodium fluoride, potassium chloride, and silver chloride did not simplify the spectrum. These experiments were done before a reliable calibration of the magnets had been accomplished and before the particle beam was made narrow enough for good resolution. Thus although some changes apparently did occur in the spectra as a result of these contaminations, no quantitative results can be given. As can be seen from the table above, the appearance of a small peak at 23, 39, or 108 might well go unnoticed even with the superior resolution obtained in later experiments.

In a few experiments, nitrogen was allowed to leak slowly into the system without effect on the spectra. When, instead of

nitrogen, oxygen was admitted, a small increase was observed in the height of the peak at mass-to-charge ratio 32. This increase persisted for several days after the introduction of the oxygen.

Coefficient measurements

Determinations were made of the average number of secondary charged particles produced by each incident positive ion. Measurements of the current of secondary positive or negative particles from a target were made with a Beckman [30] null electrometer. A small portion of the target was cut away to allow a fraction of the incident positive ions to strike the counter thus giving a measure of the total number of particles striking the target.

Figure 34 illustrates the effect of anode voltage on the number of secondary negative particles produced by each positive ion. Figure 35 illustrates the same effect on the number of secondary positive particles produced by each positive ion. When a target had been in the vacuum system for more than 24 hours, it was assumed to be "dirty". The surface of the copper-beryllium target was "dirty" with an oxide coat when it was first inserted.

Use of a Faraday cage for these experiments was made necessary by the following observations. Secondary coefficients calculated by use of grid-1 current measurements and counting

---

[30] Beckman model MX-4, National Technical Laboratories, South Pasadena, California.

FIGURE 34

SECONDARY NEGATIVE PARTICLES PER INCIDENT POSITIVE PARTICLE

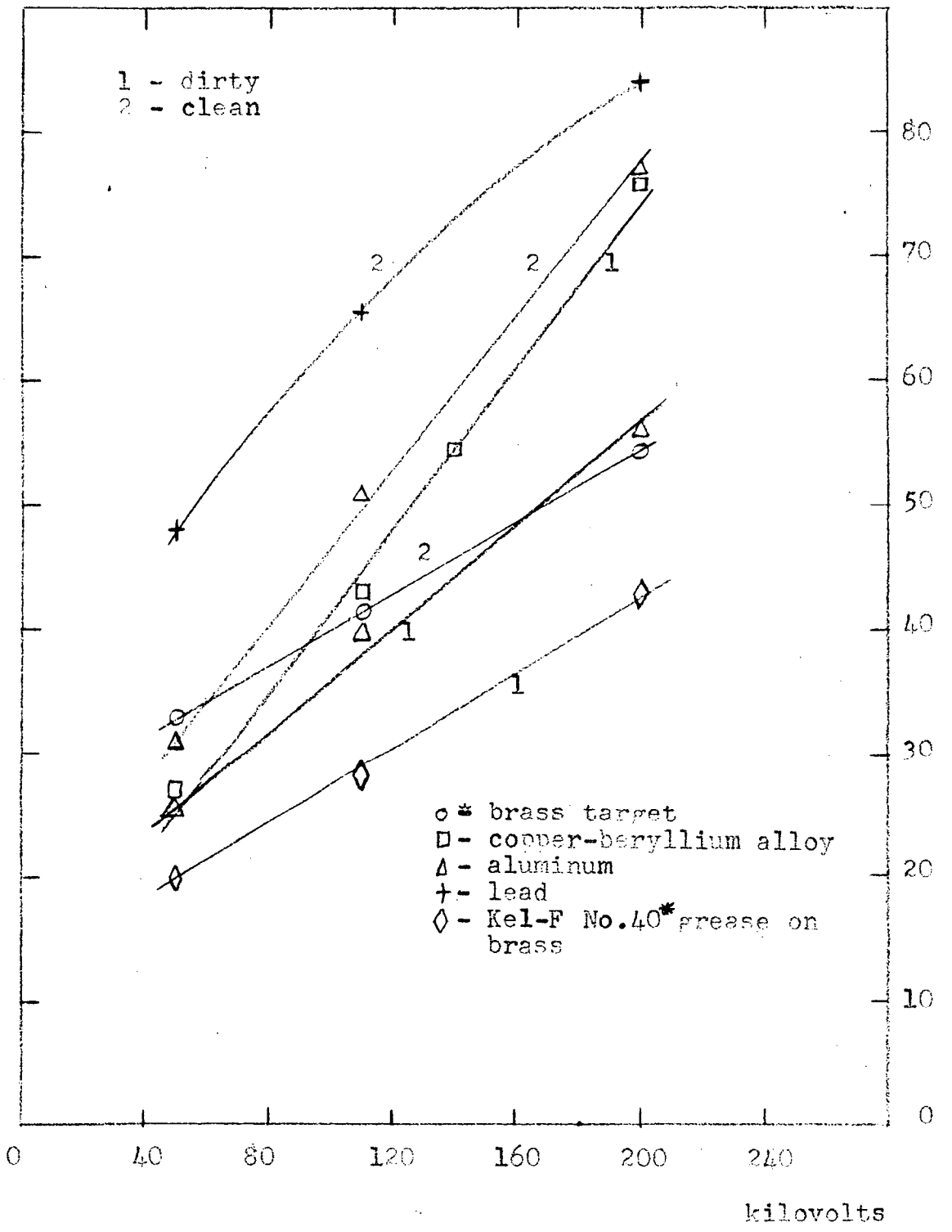

FIGURE 35

SECONDARY POSITIVE PARTICLES PER INCIDENT POSITIVE PARTICLE

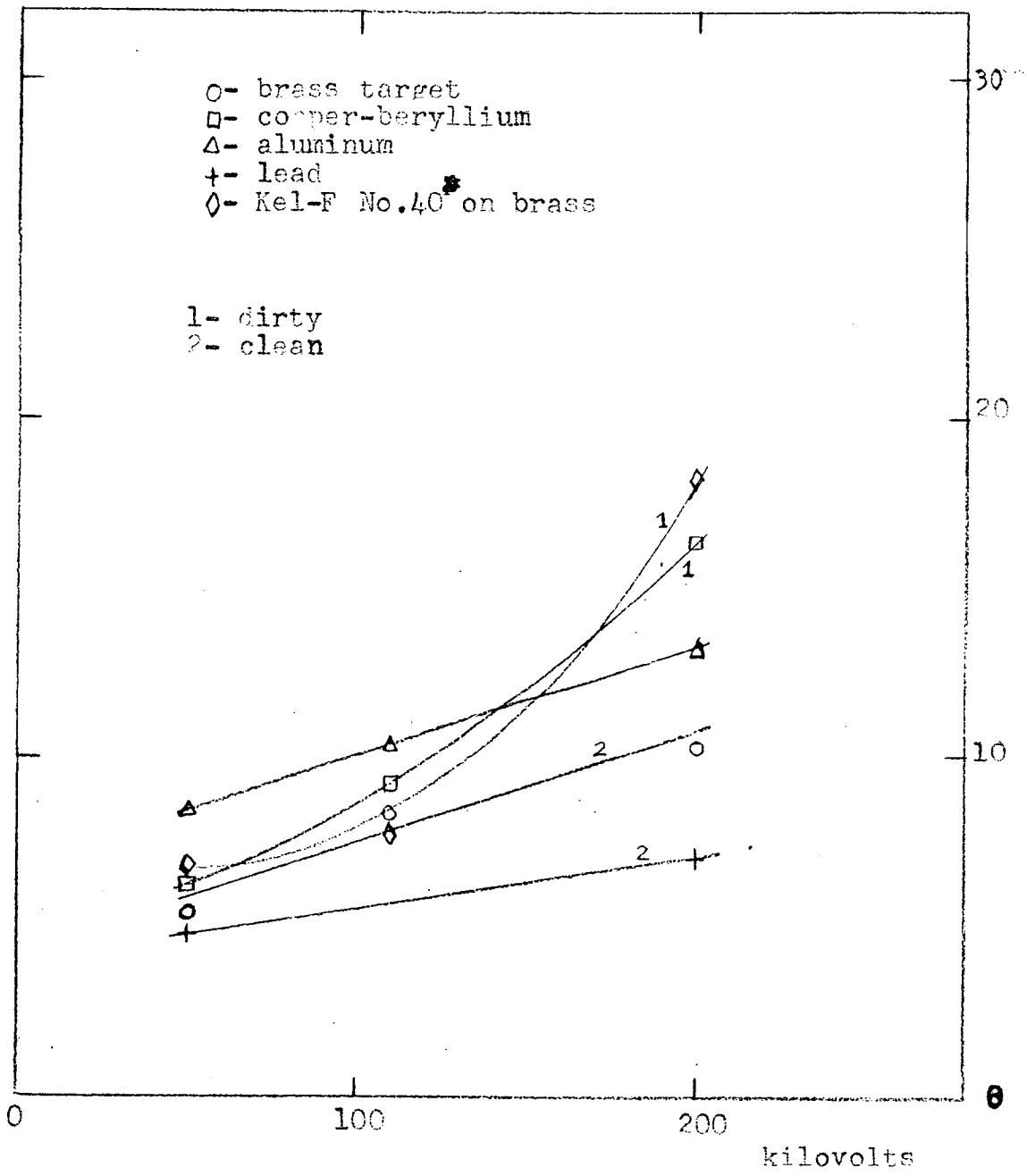

rate data were very different for the three different anodes. This was taken as an indication that the emission of positive ions from the anode surface was not isotropic. Table 5 is a resume of this effect. The solid angle subtended by the counter was 6.4×10^{-6} of the total. The slit was in the equatorial plane of the anode. It was assumed that grid-1 current represented 75 per cent of the total number of secondary negative particles minus the current required to offset the beta charging current. All results were obtained with a 180-micromicroampere source.

Table 5

Anode radius	Anode kilovoltage	Grid-1 current	Counts min^{-1}	Secondary coefficient
2 cm	60 kv	100	28,000	28.5
2	225	1000	46,000	69.5
1.25	270	1200	15,000	278
0.5	200	1800	10,000	570

The values obtained with the 4-cm anode indicate that emission from its surface is fairly uniform, since they agree with those obtained by the Faraday cage measurements. It is apparent that the rate of emission of positive ions by the 1 and 2.5-cm anodes is greater on the average than for the particular sections seen by the counter.

Attempts were made to sort the negative particles into negative ions and electrons by means of a magnetic field. The results were inconclusive in so far as the relative abundance

of negative ions is concerned. However a considerable reduction in collector current was produced by a small magnetic field perpendicular to the path from target to collector. Thus we conclude that at least a large fraction of the secondary particles are electrons.

Solenoid experiments

In a number of experiments a magnetic field of a few gauss was produced parallel to the axis of the system. The experiments were made as follows. The system was allowed to come to equilibrium at a steady limiting voltage with no magnetic field. A magnetic field was then produced by passing a current through a solenoidal winding about the vacuum system. The field was maintained until no further changes were observed, usually a matter of a few minutes. The counting rate of positive ions and the anode voltage were then recorded. Figure 36 illustrates the results of such experiments conducted with the 4-cm anode at low grid-2 bias. At higher bias the effect is still noticeable but percentagewise is smaller. For example, at a current of 6 amperes with grid-2 at -1200 volts the counting rate increased from 30,000 min^{-1} to 40,000 min^{-1}.

Results of these experiments with the 1-cm and the 2.5-cm anodes at low grid-2 bias were similar to the results with the 4-cm anode at low grid-2 bias. In the case of the 1-cm anode an increase in kilovoltage from 72 to 92 kilovolts occurred with grid 1 at 300 volts and grid 2 at 0 volts. In all other cases with all anodes no noticeable change occurred in the anode voltage when the field was turned on.

FIGURE 36

EFFECT OF A MAGNETIC FIELD ON

POSITIVE ION EMISSION

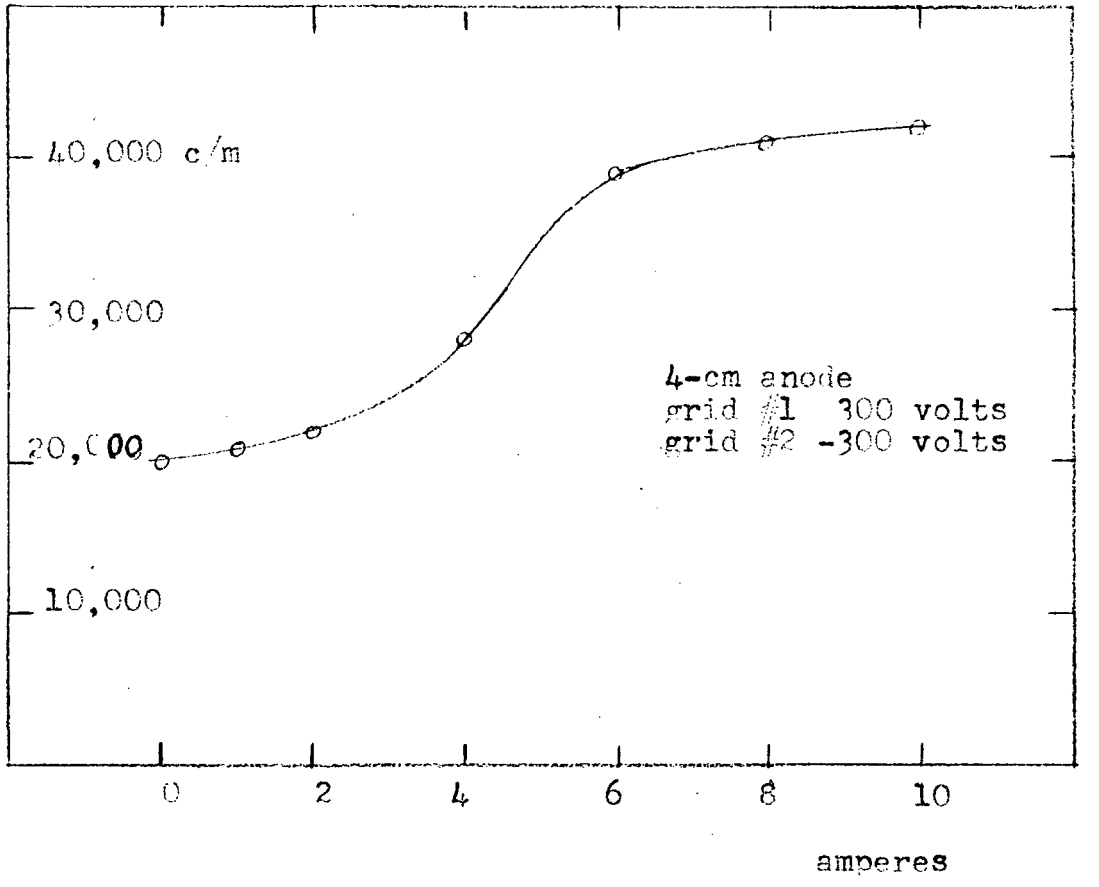

With a high bias on grid 2 the magnetic field had no effect on anode voltage or counting rate.

Phosphor experiments

A few experiments were made with a silver-activated zinc sulfide phosphor on the anode. The light produced by the bombardment of this phosphor by charged particles was observed through the glass port in the side of the metal vacuum chamber.

The intensity of the light emitted under any particular circumstances was found to depend on the thickness of the phosphor. At zero anode potential there was no visable glow except in the neighborhood of the thin aluminum window through which the beta source shines. At about 10 kilovolts a faint general glow became visible; this presumably was due to beta particles turned back by the anode voltage. With a very thin phosphor the glow did not become detectable until the anode had reached about 50 kilovolts. The glow brightened as the anode voltage increased. With a high bias on grid 2 the glow increased steadily with no sudden increases in intensity at the limiting voltage. With a low bias on grid 2 the glow brightened rapidly as the limiting voltage was attained. The three anodes produced somewhat different effects. In the following we will describe the effects for each anode separately.

The general behavior with the 4-cm anode was as described above. Occasional flashes were observed on small portions of the anode, but these were not accompanied by any measurable decrease in anode voltage. On two occasions spark discharges

were observed with the 4-cm anode. They were accompanied by very brilliant flashes covering the entire anode surface. When the solenoid was activated, a very slight decrease in intensity occurred near the top and bottom of the anode. No other effect could be detected.

In the case of the 2.5-cm anode with the grids at ground potential, the glow at limiting voltage was unsteady, flickering several times a second. These variations in intensity were not localized but included the whole phosphor surface simultaneously. Spark discharges were accompanied by brilliant flashes distributed evenly over the anode surface. Turning on the solenoid current produced a slight decrease in intensity near the top and bottom of the anode. At the same time a more intense glow appeared around the equator.

With the 1-cm anode the glow at limiting voltages appeared to be concentrated near the base of the anode, especially near the rod. The rod was coated with phosphor, in one case in bands, in another in a thin uniform coat. In both cases the phosphor on the rod glowed at limiting voltages. With an umbrella-rod the entire umbrella glowed, but no glow appeared below the umbrella. With no umbrella on the rod the glow extended about half way down the rod from the anode, the brightest glow being nearest the anode. The glow at zero grid bias was sometimes flickering, sometimes apparently steady. With grid 2 biased negatively the tendency was toward a steady glow. No steady voltages could be obtained with more than -300 volts on grid 2, apparently due to the presence of the phosphor. When grid 2 was biased at

-1200 volts or more a bright glow set in at about 70 kilovolts near the rod and on the rod. This glow increased with voltage up to about 140 or 150 kilovolts. At this point a very rapid increase in intensity was culminated by a brilliant flash and spark discharge. Turning onthe solenoid current produced a noticeable increase in intensity when grid 1 and grid 2 were at ground potential. At other biases no effect of the magnetic field was observed, with the exception of a very small decrease in intensity near the rod and a very noticeable decrease in intensity on the rod for all biases.

IV. Discussion

General

One fact is very clear as a result of this investigation. Positively charged ions are involved in all voltage limitations encountered in our system. Since each positive ion produces 20 to 80 negative particles at the cathode surface, negative particles are also involved in these limitations.

There are apparently two distinct types of dark current limitation important in our system. The first is characterized by the variation of grid-1 current with the cube of the anode voltage and with the square root of the beta charging current. The second type can be recognized by a very sudden increase in grid-1 current near the limiting voltage.

The interpretation of the current flowing to grid 1 is important in a discussion of these two types of dark current. When grid 1 is biased positively, the current flowing to the grid is positive, indicating collection of negative electricity or loss of positive electricity at the surface of the grid wires. Grid 1 has a screening fraction of 25 per cent, thus 25 per cent of the positive ions from the anode strike the grid directly and 75 per cent of the ions strike the cathode wall. The ions which strike the cathode produce negative particles which may be collected by grid 1 or may pass through the grid system to the anode. The positive ions which strike grid 1 directly produce negative particles which may or may not escape from its surface. In addition, secondary positive particles are produced both at the cathode and on grid 1. Those produced at the cathode can be collected by grid 1 only if grid 1 is

negatively biased. Those produced on the surface of grid 1 can escape either to grid 2 or to the cathode, when grid 1 is biased positively.

When grid 2 is biased at a high negative value and grid 1 is biased positively, grid 1 should collect all negative particles produced at the cathode and lose all positive particles produced at its surface. When the bias on grid 2 is not sufficiently high to protect the entire cathode from the anode field, a portion of the negative particles produced at the cathode may pass through the grid structure to the anode. Likewise, secondary negative particles from grid 1 itself may escape to the anode. Another effect becomes important under these conditions if the anode voltage is increasing. When grid 2 is not protecting the cathode, grid 1 acts as part of the cathode and as such must accumulate negative charge as the anode accumulates positive charge. The smaller current to grid 1 when grid 2 is biased at a low value is a result of these last three effects.

Assuming that the above interpretation of grid-1 current is correct, we can conclude that when grid 2 is at a sufficiently high bias, the current to grid 1 is a measure of the positive ion current emitted from the anode surface. Using average curves from figures 34 and 35, we deduce this relation between positive ion current and grid-1 current: $I_1 = (0.164\ V + 12.25)\ I_+$. Here I_1 is the current to grid 1 in micromicroamperes, V is the anode voltage in kilovolts, and I_+ is the positive ion current from the anode in micromicroamreres.

According to figure 25, the current drawn by grid 1 is proportional to the square root of the source strength when grid 2 is biased at a high negative voltage. This relationship implies that the beta particles themselves are in some manner responsible for the positive ions emitted from the anode.

At any given voltage, the number of beta particles striking the anode surface is just proportional to the source strength. All the beta particles pass through a portion of the surface as they shine out from the internally mounted source. Some of the beta particles are turned back by the anode field and strike the anode surface at least once again. (See figure 3.) If the beta particles produced positive ions and if these ions escaped from the surface immediately after formation, then the positive ion current would be proportional to the first power of the source strength. If the ions formed on the surface escaped only slowly and were eliminated primarily by bimolecular recombination reactions, then the positive ion current would be proportional to the square root of the source strength.

This occurs in the following manner. Let c_+ and c_- be the concentrations of positive and negative ions on the anode surface. It is assumed that these ions are formed by the passage of electrons through a layer of organic material (oil) on the surface of the anode. Let R_f be the rate of formation of these ion pairs and R_d the rate of disappearance. At equilibrium, R_f must be equal to R_d. R_f is proportional to the electron current striking the anode, I_e. If most of the positive ions disappear by recombination with negative ions, then R_d is proportional to the product of the concentrations

(number per unit area) of positive and negative ions and the area of the surface, A. If it is further assumed that the concentrations of the positive and negative ions cannot differ greatly, then R_d can be expressed as $R_d = k_1(c_+)^2A$. Setting R_d equal to R_f we obtain the expression $c_+ = k_2(I_e/A)^{\frac{1}{2}}$. Then if the rate of escape of positive ions is proportional to the concentration of positive ions, we obtain the required relationship $I_+ = k_3(AI_e)^{\frac{1}{2}}$. Here I_+ is the total positive ion current from the entire anode surface.

The electron current striking the anode surface comes from three sources. Two of these, the beta particles passing through the surface from an internal source and the beta particles returning to the anode because of the anode field, give rise to electron currents directly proportional to the source strength. Positive ions striking grid 2 produce electrons (and possibly negative ions) which can in turn strike the anode surface. The electron current from this latter source is proportional to the positive ion current (and therefore to the square root of the source strength, I_{b0}). Thus $I_e = k_4I_{b0} + k_5(I_{b0})^{\frac{1}{2}}$. The electron current from the grid wires is never more than the source strength minus the returning beta current, so I_e can be approximated by an expression $I_e = k_6(I_{b0})^n$ where n is some number slightly less than one. Experimentally, the relationship between the positive ion current and the source strength is best fitted by an expression $I_+ = k_7(I_{b0})^{0.44}$. Substitution of $k_6(I_{b0})^{0.88}$ for I_e in the expression $I_+ = k_3(AI_e)^{\frac{1}{2}}$ gives the expression $I_+ = k_3(Ak_6)^{\frac{1}{2}}I_{b0}^{0.44}$. Thus the above hypothesis is consistent with experimental results.

With two exceptions the forces affecting a positive ion imbedded in a dielectric film which covers a positively charged metal surface are the same as those affecting a neutral molecule in the same position. These two exceptions are the coulombic repulsion due to the charge on the metal surface and the attractive "image force" due to polarization of the charge distribution in the metal surface. Thus a positive ion may be expected to desorb (evaporate) just as neutral molecules are doing, with the exception that the rate of desorption will be modified by the forces mentioned.

In the Glasstone, Laidler, and Eyring treatment an expression for the rate of desorption per unit area is derived:

$$R_d = \frac{B}{r}\frac{kT}{h} e^{-E/RT} \qquad (1)$$

where B is the fraction of the surface covered, r is the area occupied by an adsorbed molecule, h is Planck's constant, k is Boltzman's constant, R is the gas constant, T is the absolute temperature, and E is the activation energy for desorption. If it is assumed that there is no activation energy of adsorption, E may be approximated by the heat of condensation.

In our system we can assume that the entire anode surface is covered with adsorbed molecules. Then to calculate the rate of desorption of positive ions we must use for $\frac{B}{r}$ the concentration of ions on the surface. The quantity E will be the heat of condensation for the molecular ions, modified by the image and the coulombic forces.

The positive ion emission from the anode should have the form

$$\frac{I_+}{A} = k_2\left(\frac{I_e}{A}\right)^{\frac{1}{2}} \frac{kT}{h} e^{-\frac{(E+E_i-E_f)}{RT}} \quad , \qquad (2.)$$

where $k_2\left(\frac{I_e}{A}\right)^{\frac{1}{2}}$ is the concentration of positive ions (see page 80), E is the heat of vaporization, E_i is the energy required to overcome the image force, and E_f is the energy supplied by the coulomb force during desorption. This equation may be rewritten in the form

$$I_+ = \beta(AI_e)^{\frac{1}{2}} e^{2.3\times10^{7}\gamma E_a} \quad , \qquad (3.)$$

where $\beta = k_2 \frac{kT}{h} e^{-\frac{(E+E_i)}{RT}}$ is assumed to be a constant in our system. The term γ is the distance in centimeters through which an ion moves during desorption, and E_a is the electric field at the anode in volts cm^{-1}.

The experimentally determinedd positive ion current from the 1-cm anode at high grid-2 bias can be expressed as a function of voltage and electron current in an equation of the above form. The equation is

$$I_+ = 0.0665(A)^{\frac{1}{2}}(\alpha I_{bo} + I_{br} + I_{es})^{\frac{1}{2}} e^{6.75\times10^{-6}E_a} . \qquad (4.)$$

In this equation A is the area in square centimeters, I_{bo} is the zero-kilovoltage charging current in micromicroamperes, I_{br} is the zero kilovoltage charging current minus the charging current at voltage (estimated from figure 3), and I_{es} is the secondary electron current from the grid wires in micromicroamperes (estimated from the screening fraction and grid-1 current). The quantity E_a is the anode field calculated assuming spherical geometry. The constant α is a number estimated in the following manner. The beta particles from

the internal source pass out through about one half of the anode surface. Since the concentration of positive ions is assumed to vary with the square root of the electron current density, the concentration on this half of the anode will be $\sqrt{2}$ time the concentration which would be produced if the beta particles were distributed over the entire surface. The effect is that the average concentration is $\frac{\sqrt{2}}{2} = 0.7$ as great as it would have been with isotropic distribution. Using the same argument we obtain $\frac{\sqrt{20}}{2^4} = 0.22$ and $\frac{\sqrt{50}}{5^4} = 0.14$ respectively as values of α for the 2.5 and 4-cm anodes.

Equation 4 was derived from experimental data for the 1-cm anode at voltages above 100 kilovolts. Below this voltage the measured currents fall below values calculated from the equation. The value of 6.75×10^{-6} for the coefficient of the anode field in the exponential term corresponds with a distance of 17.5 angstroms.

An estimate can be made of the number of positive ions which might be formed in a film of grease by the passage of an electron through that film. Assuming that the film is composed of di-octyl sebacate (Octoil-S) in a monomolecular layer, the film should be about 15 angstroms thick. A 100-kev electron forms about 150 ion pairs mg^{-1} cm^2. Thus in a single pass through the film such an electron should make 0.0225 ion pair on the average. About 40 per cent of the electrons which enter the film backscatter from the anode surface. These backscattered electrons will have a lower energy and therefore a much higher specific ionization. The scattered electrons, once outside the film, will be drawn back to the anode by the coulomb attraction

of the anode field. These effects may increase the yield of ion pairs by a factor of 4. Another factor which must be considered is the angle at which the electron impinges on the surface. Because the above number was estimated on the assumption of normal incidence, it should be roughly doubled to take account of random angles of incidence. Thus as a crude estimate the average electron may be responsible for 0.2 ion pair in the monomolecular surface film.

Consider the case of the 1-cm anode at 150 kilovolts with a 50-micromicroampere source. Grid 1 draws 273 micromicroampere indicating a positive ion current of 7.4 micromicroampere (see page 78). Thus the current density of positive ions at the anode is 1.5×10^{7} $sec^{-1}cm^{-2}$, and the current density of electrons at the anode is 4×10^{8} $sec^{-1}cm^{-2}$. This electron current might produce 8×10^{7} positive ions $sec^{-1}cm^{-2}$. These estimates indicate that about 80 per cent of the ions can disappear by recombination reactions, leaving about 20 per cent to escape by evaporation.

An estimate can also be made of the concentration of ion pairs on the anode surface. This requires some assumption as to the value of the heat of evaporation for the positive ions. For a molecule like di-octyl sebacate this might be close to 20 kcal $mole^{-1}$. Most of the positive ions are less than half the size of this molecule so we will chose for trial a value of 10 kcal $mole^{-1}$. With the assumption that the ion starts desorption at a point 8 angstroms from the metal surface of the anode and becomes free at a distance of 25 angstroms,

the "image" force adds 7 kcal $mole^{-1}$, and the coulombic repulsion subtracts 1.2 kcal $mole^{-1}$ from this value. With an estimate of about 50 square angstroms for r, we obtain for B a value of 5×10^{-9}. Here B represents the fraction of the surface molecules which are positive ions. Then c_+ is about 1×10^6 positive ions cm^{-2}. This implies that equilibrium is attained in a small fraction of a second, because the rate of loss of positive ions is ten times this number per second. Of course, the above calculation is extremely sensitive to the estimate of the heat of vaporization, and the result should be taken as illustrative rather than conclusive.

The relatively large fraction, 20 per cent, of the positive ions which must escape according to the above calculation makes it seem likely that there is some additional process producing positive ions when grid 2 is at a high negative bias. On the other hand, any process which depends on the production of cathodic particles by the positive ions which escape by evaporation would be incompatible with the experimental square root law (see page 79). A tentative position is that although there may be some multiplication of the positive ion current by the action at the anode of secondary cathodic particles, such a process can hardly be responsible for more than about half of the current under these conditions.

The equation for positive ion emission from the 1-cm anode does not fit the curves obtained for the 2.5 and 4-cm anodes at high grid-2 bias. Currents calculated from equation (4) are two to three times too high at about 100 kilovolts. At the limiting voltages values from equation (4) agree within about 30 percent for all anodes. Table 5 summarizes these results for the 2.5 and 4-cm anodes.

Table 5

Anode diam.	Source strength	Voltage	Grid-1 current	
			calculated	measured
2.5 cm	50 μμamp.	225 kv	388 μμ amps	300 μμ amp.
4	180	225	635	670
4	50	202	330	250

We will return to the discussion of equation (4) after a discussion of the dark current observed with low bias on grid 2.

As we have noted, when the bias on grid 2 is below the critical value, the current produced at the cathode by incident positive ions rises very sharply as the anode voltage nears the limiting value. This behavior suggests an exchange mechanism as the cause of voltage limitation. The finite slope of current versus voltage curves suggests a current-dependent exchange.

We believe that such an exchange type of mechanism is responsible for voltage limitations at low grid biases. In the following paragraphs we will show that our data are consistent with an exchange mechanism involving both electrons and negative ions as the cathodic particles. We will also show that emission of positive ions by evaporation from the anode surface is consistent with our data.

In a pure exchange mechanism, particles are produced at an electrode only by the impact of particles from the other electrode. However, in our system the beta source provides a continuous supply of positive ions on the anode surface. Thus we can regard all leakage currents which depend on positive ions as a multiplication of the current produced by the beta particles.

Such a multiplication of current can not supply the leakage currents observed at low grid-2 biases, if only electrons are produced at the cathode. At a low limiting voltage with grid 2 at a low bias the electron current striking the anode can be no greater than the zero-kilovoltage charging current. At the same anode voltage with a high grid bias the electron current is less, but, due to returning beta particles, it is certainly no less than one tenth at any observed limiting voltage. According to the theory of evaporation of positive ions, a ten fold increase in electron current should produce a 3.16 ($\sqrt{10}$) fold increase in positive ion emission. In the case of the 4-cm anode, we have observed a positive ion current 100 times as great at low bias as at high bias. Thus we conclude that cathodic particles other than electrons must be responsible for a large fraction of the multiplication at low grid-2 bias. We believe that these particles are negative ions.

The results of the solenoid experiments support the theory that negative ions are the primary producers of anodic positive ions when the anode voltage is limited with low grid-2 bias. A magnetic field parallel to the axis of the system caused an increase in the rate of positive ion emission. The field presumably reduced the fraction of the secondary cathodic electrons which could reach the anode. Multiplication of the positive ion current by a positive ion—negative ion exchange increased until the reduction in electron current was compensated for by positive ions, negative ions, and an increase in the number of secondary electrons produced at the cathode. The negative ions, with

mass-to-charge ratios thousands of times larger than that for electrons, were not affected appreciably by the magnetic field.

We believe that positive ions formed by either electrons or negative ions are subject to recombination reactions on the anode surface. The evidence for this in the case of those ions formed by electrons has already been presented. In the case of positive ions formed by negative ions the theory of evaporation is supported by observation of a change in the apparent coefficient product, c_1c_2, with anode diameter. The derivation and interpretation of this effect is complex, and only a brief discussion is presented here. A more complete discussion is presented in appendix A.

If it is assumed that all positive ions produced by negative ions escape immediately from the anode surface, then the multiplication due to a positive ion—negative ion exchange can be expressed as $1/(1-fc_1c_2)$. The quantity f is defined as the fraction of the total number of negative ions produced at the cathode which can reach the anode. The quantities c_1 and c_2 are the coefficients for production of negative ions at the cathode and positive ions at the anode by the impact of positive ions and negative ions respectively. Table 6 illustrates the effect of anode diameter on the product c_1c_2.

Table 6

Anode diameter	Source strength	Grid-2 bias	Anode voltage	f	$c_1 c_2$
4 cm	50 amp.	-1200 v	150 kv	0.098	8.95
4	50	-600	110	0.162	5.85
1	50	-300	120	0.098	1.8

The changes in coefficient product with anode size are consistent with the theory that positive ions escape from the anode surface by an evaporative process and disappear primarily by recombination reactions. The larger anode has a larger surface area, and therefore at the same anode field fewer positive ions cm^{-2} are required to produce a given positive ion current. The lower concentration means that a smaller fraction of the ions will undergo recombination reactions in a given time, thus a larger fraction will escape by evaporation. This results in a larger value of the coefficient c_2 for the larger anode.

We believe that the effects observed with the 2.5 and 4-cm anodes at limiting voltages and high grid-2 bias are due to a multiplication of the electron induced emission by a negative ion—positive ion exchange. We will discuss the reasons for this conclusion, but first we must discuss the deviations of the experimentally determined positive ion emission for the 2.5 and 4-cm anodes from the empirical equation derived from the results obtained with the 1-cm anode.

As was noted before, equation (4) does not correctly predict the positive ion emission for the 2.5 and 4-cm anodes at voltages below the limiting kilovoltage. However, an equation of the same

form as equation (4) with 0.02 substituted for 0.0665 as the value of β does fit the experimental results up to voltages of about 200 kv and 180 kv respectively for the 2.5 and 4-cm anodes. There are several possible reasons for this difference. The surface area of the anode proper was used for A in equation (4), but the umbrella and rod as well as the anode were found to be emitting positive ions. Use of a larger value for A would reduce the required value for β. The concentration of positive ions on the 1-cm anode may be enhanced by a positive ion—negative ion exchange with the umbrella. There is also a question as to the validity of the derivation of the constant α. All of these effects tend to produce a value of β which is too high, thus we conclude that β should be approximately 0.02 for all anodes. We must then regard the approximately correct predictions of emission in table 5 as coincidental, and we must find an explanation for an increase in emission at limiting voltages.

At limiting voltages with high grid-2 bias the emission of positive ions from the 2.5 and 4-cm anodes is no longer proportional to the square root of the charging current as it is at lower voltages. As we noted on page 80, the production of positive ions by secondary cathodic particles tends to mask the square root law. Thus the deviation from the square root law may be due to a negative ion—positive ion multiplication. The appearance of this multiplication in the case of the 2.5 and 4-cm anodes and the lack of it in the case of the 1-cm anode may be due to a more favorable value of c_2^2 in the case of the larger anodes. This would result from a lower concentration of positive ions and thus

a larger probability for any particular ion to escape.

We now have a general picture of the mechanisms by which leakage currents of the "dark current" type are produced in our system. There are two mechanisms, one of them peculiar to our system in that it results from the presence of a beta source in the anode. In both mechanisms, positive ions are formed in a film on the surface of the anode. These ions undergo recombination reactions, and only a fraction of them escape from the surface.

There are a number of phenomena which have not been discussed. In the following we will discuss a number of these briefly.

Dependence of coefficient on field

There is evidence that the coefficient for production of electrons at grid 2 is dependent on the magnitude of the electric field at the grid wires. At a limiting voltage of 170 kilovolts on the 1-cm anode, the leakage current requires a secondary coefficient of 51 electrons per incident positive ion at the grid wires. This is comparable with the numbers obtained as secondary coefficients with the Faraday cage (figure 34). When the 4-cm anode is limited at 200 kilovolts, one has to assume a coefficient of 112 electrons per incident ion to explain the negative leakage current. The fields at the grid wires in these two cases were 10 kv cm^{-1} for the 1-cm anode and 54 kv cm^{-1} for the 4-cm anode.

T. J. Lewis[14] describes a "Malter-like" effect which is important for fields of the order of 10^5 volts cm^{-1}. It seems likely that some such effect is the cause of the increase in coefficient at the grid wires for fields of about 5×10^4 volts cm^{-1}.

Dissociations

The appearance of a "neutral" peak in the mass spectra of positive ions can be explained only by dissociation of positive ions, in flight, into charged fragments and neutral fragments. The peaks at mass-to-charge ratios of 0.65, 1.4, etc. can be explained on the basis of dissociation in flight. The transit time for a positive ion is of the order of ten's of microseconds, thus the parent ions must have a mean life of about the same order of magnitude. The peaks at apparent mass-to-charge ratios 0.65, 1.4, etc. are due to dissociations which occur after the ions have traversed the electric field but before they reach the magnetic field.

Spark discharge

The spark discharges in our system seem to be intimately related to the presence of positive ions on the anode surface. Perhaps a discharge occurs when the coefficient product, fc_1c_2, momentarily exceeds unity. The size of the discharge would be determined by the extent to which fc_1c_2 is greater than 1. The "bursty" count rate and the flickering of a phosphor on the anode suggest that at low grid-2 bias the positive ion concentration is fluctuating several times a second. The steady count rate at high grid-2 bias is a result of the continuous production of positive ions by the steady beta current.

Double pulses

The double pulses mentioned in the experimental results section may be due to negative ions produced at the first dynode of the electron multiplier. An incident ion might produce 50 secondary

electrons and one negative ion. The electrons would reach the second dynode before the negative ion. If the negative ion produced a few electrons at the second dynode, the result would be a double pulse with the second peak somewhat smaller than the first.

Time delay in positive ion emission

The observation of a delay of about 1 millisecond in the stopping of positive ion emission, when the bias on grid 2 is increased suddenly, lends strong suprort to the theory of positive ion evaporation. The lack of sufficient data prohibits the use of this observation for anything more than corroborative evidence.

Higher voltages

As a result of this investigation, several suggestions can be made concerning methods for increasing the maximum obtainable voltages in a system similar to ours. One obvious step should be the elimination of all sources of organic contaminants. This in itself might eliminate the possibility of leakage due to electrons from the beta source; however reduction in the area exposed to beta radiation might also be worthwhile. A larger system would permit the use of a cathode grid while reducing leakage of the Malter type and more generally, all types of field sensitive electron emission.

V. SUMMARY

We have investigated the leakage of electricity across a vacuum space in an oil-pumped vacuum system. The leakage has been shown to consist of a flow of positive and negative particles between the anode and the cathode. The positive particles were found to be primarily organic ions produced in a layer of oil on the surface of the anode. The negative particles were shown to be mostly electrons.

We have measured the yields of secondary negative particles and secondary positive particles produced by average positive ions in the energy range from 50 to 200 kev. These yields were found to be dependent on the nature of the target material as well as on the energy of the incident ion.

A mass spectrometer was employed to study the nature of the positive ions. Most of these ions were charged fragments of organic molecules with masses ranging from 1.0 atomic mass unit to more than 1000 atomic mass units. The most prominent peaks in the mass spectra occurred at mass-to-charge ratios of 27, 32, and 46. Neutral particles were attributed to dissociation of a portion of the positive ions during their flight from anode to cathode.

We have proposed two mechanisms to explain our experimental results, both involving the formation of positive ions in the film of organic material covering the anode surface. Electrons, most of which originate at the beta source, are presumed to be the agent for positive ion production in one mechanism,

Multiplication of the electron-induced positive ion current by a negative ion—positive ion exchange can be expressed as $1/(1-fc_1c_2)$, if the positive ions produced by negative ions escape from the anode surface immediately. This expression was derived as follows. Assume each positive ion on the average causes c_1 negative ions to be emitted and each negative ion on the average causes c_2 positive ions to be emitted. Assume that fc_1 of the negative ions strike the anode. An initial positive ion makes fc_1c_2 positive ions which then produce $(fc_1c_2)^2$ positive ions etc. The multiplication factor is then the sum of an infinite series, $1 + fc_1c_2 + (fc_1c_2)^2 + \ldots (fc_1c_2)^n \ldots$. If fc_1c_2 is less than one, this series is equal to $1/(1-fc_1c_2)$.

The value of the multiplication factor can be calculated from experimental results. Measurements of the current to grid 1 at a given voltage, first with high bias then with low bias, provide the necessary data. The multiplication factor is the ratio of positive ion emission at low bias to that at high bias. The values of c_1c_2 recorded in table 6 were obtained by equating the multiplication factor and the expression $1/(1-fc_1c_2)$.

We have calculated values for the coefficient product, c_1c_2 (table 6), on the assumption that the positive ions produced by negative ions escape immediately from the anode surface. We will now use equations (1) and (4) in an attempt to predict the ratio of c_1c_2 for the 4-cm anode to c_1c_2 for the 1-cm anode. We will assume that a reasonable agreement between the calculated value and the predicted value of this ratio is an indication that the positive ions produced by negative ions are subject to the same

recombination and evaporative processes as those produced by electrons.

The ratio of c_1c_2 for the 4-cm anode to c_1c_2 for the 1-cm anode can be expressed in terms of probability of escape for positive ions on the anode surface. The probability that a positive ion on the anode surface will escape by evaporation is given by the expression $P = R_d/R_r + R_d$, where R_d is the rate of desorption of positive ions and R_r is the rate of recombination. If R_d is less than R_r, the approximation $P = R_d/R_r$ can be made. From equations (1) and (4) in the discussion we get the relationships $I_+ = AR_d = kTh^{-1}Ac_+ e\{\exp 6.75 \times 10^6 E_a\}$, where A is the area of the anode, c_+ is the concentration of positive ions, and E_a is the anode field in volts cm^{-1}. The quantity R_r is by hypothesis proportional to $(c_+)^2$. With the assumption that c_1 is independent of cathode field, the ratio of c_1c_2 for the 4-cm anode to c_1c_2 for the 1-cm anode is given by the equation

$$\frac{c_1c_2(4)}{c_1c_2(1)} = \frac{P(4)}{P(1)} = \frac{c_+(1)}{c_+(4)} \; e\{\exp 6.75 \times 10^{-6}[E_a(4) - E_a(1)]\}.$$

In this equation the numbers in parentheses refer to anode diameter. The value of the exponential term depends only on the voltages and radii of the two anodes. The ratio of $c_+(1)$ to $c_+(4)$ can be obtained from experimental data, if we assume the validity of equations (1) and (4). The secondary negative current to grid 1 is used in the usual manner to calculate the positive ion emission rates, $I_+(1)$ and $I_+(4)$. The quantity $I_+(1)/I_+(4)$ is equal to the expression

$$\frac{I_+(1)}{I_+(4)} = \frac{c_+(1)\; A(1)}{c_+(4)\; A(4)} \; e\{\exp 6.75 \times 10^{-6}[E_a(1) - E_a(4)]\}.$$

Solving this for $c_+(1)/c_+(4)$ and substituting in the above

equation we obtain the following form for the ratios of coefficient products;

$$\frac{c_1c_2(4)}{c_1c_2(1)} = \frac{I_+(1)}{I_+(4)} \quad \frac{A(4)}{A(1)} \quad e\left\{\exp 2 \times 6.75 \times 10^{-6}\left[E_a(4) - E_a(1)\right]\right\}.$$

Substitution of experimental data obtained for the 4-cm anode at 150 kv with -1200 volts on grid 2 and for the 1-cm anode at 120 kv with -300 volts on grid 2 gives $c_1c_2(4)/c_1c_2(1) = 5.9$. This is in satisfactory agreement with the ratio of the values in table 6: $c_1c_2(4)/c_1c_2(1) = 5.0$. Thus we conclude that evaporation and recombination reactions are important fro positive ions produced by negative ions.

APPENDIX B

Bibliography

Allen, J. S., "The Secondary Emission of Electrons Due to Protons," Phys. Rev. 55, 236A (1939).

Allen, J. S., "An Improved Electron Multiplier," Rev. Sci. Instr. 18, 739 (1947).

Arnot, F. L. and Beckett, C., "Formation of Negative Ions at Surfaces," Nature 141, 1011 (1938).

Bailey, T. L., McGuire, J. M., and Muschlitz, E. E., Jr., "Formation of Negative Ions in Hydrocarbon Gases," J. Chem. Phys. 22, 2088 (1954).

Bethe, H. A., "The Range-Energy Relation for Slow Alpha-Particles and Protons in Air," Rev. Mod. Phys. 22, 213 (1950).

Bourne, H. C., Cloud, R. W., and Trump, J. G., "The Role of Positive Ions in High Voltage Breakdown in Vacuum," J. Appl. Phys. 26, 596 (1955).

Cranberg, L., "The Initiation of Electrical Breakdown in Vacuum," J. Appl. Phys. 23, 518 (1952).

Dycke, W. P. and Trolan, J. K., "Field Emission: Large Current Densities, Space Charge, and the Vacuum Arc," Phys. Rev. 89, 799 (1953).

Fowler, R. H. and Nordheim, L., "Electron Emission in Intense Electric Fields," Proc. Roy. Soc. A119, 173 (1928).

Glasstone, S., Laidler, K. J., and Eyring, H., "The Theory of Rate Processes, " McGraw-Hill Book Co., New York (1941).

Graggs, J. D., McDowell, C. A., and Warren, J. W., "Electron Capture Processes in Polyatomic Molecules," Trans. Faraday Soc. 48, 1093 (1952).

Lewis, G. N. and Lipkin, D., "Reversible Photochemical Processes in Rigid Media: The Dissociation of Organic Molecules into Radicals and Ions," J. Am. Chem. Soc. 64, 2801 (1942).

Lewis, T. J., "The Mechanism of High Field Emission of Electrons from Tarnished Metal Surfaces," Proc. Roy. Soc. 68B, 504 (1955)

Linder, E. G., "Nuclear Electrostatic Generator," Phys. Rev. 71, 129 (1947).

Linder, E. G. and Christian, S. M., "The Use of Radioactive Materials for the Generation of High Voltages," Phys. Rev. 83, 233A (1951).

Linder, E. G. and Christian, S.M., "The Use of Radioactive Materials for the Generation of High Voltages," J. Appl. Phys. 23, 1213 (1952).

Malter, L., "Anomalous Secondary Electron Emission, A New Phenomenon," Phys. Rev. 49, 478 (1936).

Malter, L., "Th in Film Emission," Phys. Rev. 50, 48 (1936).

Marcus, R. A., "Lifetimes of Active Molecules," J. Chem. Phys. 20, 352 (1952).

Massey, H. S. W., "Negative Ions," Cambridge University Press, Cambridge, (1950).

Massey, H. S. W. and Burhop, E. H. S., "Electronic and Ionic Impact Phenomena," Oxford University Press, London (1952).

McKibben, J. L. and Boyer, K., "Current Loading in Ion Accelerating Tubes," Phys. Rev. 82, 315A (1951).

Merten, U., "Anode Surface Effects in Conduction through a Vacuum," Ph.D. Thesis, Washington University (1955).

Miller, P. H., Jr., "A New Type of Electrostatic Generator," Phys. Rev. 69, 666 (1946).

Moseley, H. G. J., "The Attainment of High Potentials by the Use of Radium," Proc. Roy. Soc. A88, 471 (1913).

Müller, E. W., "Das Feldionenmikroskop," Zeitschrift fur Physik, Bd. 131, S. 136-142 (1951).

Murphy, P. V., "A Preliminary Study of the Effect of Cathode Surface and Configuration on the Leakage Current through a Vacuum," A. M. Thesis, Washington University (1954).

Pritchard, H. O., "The Determination of Electron Affinities," Chem. Rev. 52, 529 (1953).

Sloan, R. H. and Press, R., "The Formation of Negative Ions by Positive Ion Impact on Surfaces," Proc. Roy. Soc. A168, 284 (1938).

Sloan, R. H. and Love, H. M., "The Formation of Li^- from Li^+ at a Surface," Nature 159, 302 (1947).

Strutt, Hon. R. J., "An Experiment to Exhibit the Loss of Negative Electricity by Radium," Phil. Mag. VI, 588 (1903).

Smith, L.G., "Ionization and Dissociation of Polyatomic Molecules by Electron Impact. I, Methane," Phys. Rev. 51, 263 (1937).

Trump, J. G. and Van de Graaff, R. J., "The Insulation of High Voltages in Vacuum," J. Appl. Phys. 18, 327 (1947).

Turner, C. M., "Electron Loading in Ion Accelerating Tubes, I," Phys. Rev. 81, 305A (1951).

Van Atta, L. C., Van de Graaff, R. J., and Barton, H. A., "A New Design for a High-Voltage Discharge Tube," Phys. Rev. 43, 158 (1933).

Webster, E. W., Van de Graaff, R. J., and Trump, J. G., "Secondary Electron Emission from Metals under Positive Ion Bombardment in High Extractive Fields," J. Appl. Phys. 23, 264 (1952).